



Escuela Superior de Tecnología y Ciencias Experimentales

Instituto de Tecnología Cerámica

STUDY OF THE GRINDING PROCESS OF A RAW MATERIAL OF CERAMIC NATURE

DEGREE FINAL PROJECT

Rafael Pallarés Monserrat

Directed by:

Vicente Sanz Solana

Juan Vicente Sancho Llopis

Castellón, September 2016

Index

| | |
|--|----|
| ABSTRACT | 5 |
| ACKNOWLEDGMENTS | 7 |
| 1. INTRODUCTION | 9 |
| 2. OBJETIVES | 20 |
| 3. EXPERIMENTAL SECTION | 21 |
| 3.1. Experimental Design | 21 |
| 3.2. Components of Ink | 22 |
| 3.3. Control Variables and Compositions | 23 |
| 3.4. Preparation of Compositions of Unpigmented Inks | 24 |
| 4. RESULTS AND DISCUSSION | 27 |
| 4.1. Results | 27 |
| 4.2. Mathematical Model Adjustment and Interpretation of Results | 31 |
| 4.3. Optimal Composition of Experimental Design | 43 |
| 4.4. Results of the Optimal Composition and Interpretation | 44 |
| 5. CONCLUSIONS | 45 |
| SUPPLEMENTARY MATERIAL | 46 |
| 1. Characterization of Particle Size Distribution | 46 |
| 2. Characterization of Rheological Behavior | 47 |
| 3. Characterization of Stability against Sedimentation | 49 |
| 4. Characterization of Surface Tension | 53 |
| 5. Characterization of Density | 54 |
| REFERENCES | 55 |

ABSTRACT

In this degree final project, I have been working with Technology Ceramic Institute of the University Jaume I of Castellón de la Plana.

In recent years, the form of decoration of ceramic tiles has completely changed. The apparition of the first decorating ceramic tiles machine which used digital inkjet technology revolutionized the ceramics sector.

These developments have made a necessary remodeling in the traditional inks and their properties to adapt them to the required ones for this new type of applications.

In this project, a review of digital inkjet technology will be done and different formulations of ink with alumina will be studied as preliminary studies in order to get a matt effect.

ACKNOWLEDGMENTS

I would like to express my appreciation to all those who provided me with the possibility to complete this report.

First of all, I would like to thank both Vicente Sanz and Francisco Rodriguez for giving me the opportunity to do this project in ITC. I would like to thank Vicente Sanz for your attention and to follow up in every moment of my project.

On the other hand, and no less important, I would like to thank Adriana Belda and Javier Castellano by coordinate of this present project, for given knowledge and for all aid received.

I would like to express my gratitude to ITC for the treatment received.

And finally, I would like to thank my family and my friends for all support received.

1. INTRODUCTION

The **digital inkjet** is a printing technique which uses a non-contact process.¹

The digital inkjet printing technology appeared in the ceramics industry in 1999 through the **KERAJet** Company. Its main objective was the industrial production of the first prototype of inkjet machine for **decorating ceramic tiles**.

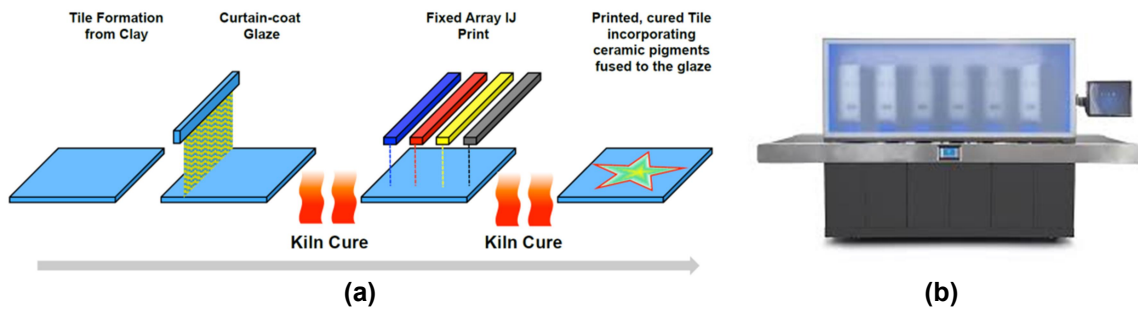


Figure 1-1. (a) Schematic of ceramic tile manufacture & decorating and (b) Ceramic tile printers: KERAjet

But it was not until 2007, when digital tile decoration really broke through and became process which is today. It was due to appearance of the Xaar 1001 printhead and its integrated ink recirculation technology.² Although KERAjet began with this one; there are others main manufacturers of ceramic tile printers like Durst or Cretaprint.

The digital inkjet appeared in order to improve the limitations of traditional processes such as:

Screen printing is a printing technique used in the method of reproduction of documents and images on any material. This technique consists of transferring an ink through a stretched mesh in a frame, the ink passage is blocked in areas where there is not image using an emulsion or varnish, leaving free the area through which the ink will pass, thus obtaining the desired image on the tile.

Gravure is a printing technique in which images are transferred to the tile from a surface whose depressions containing ink. To do this, the impression cylinder is immersed in the inkpot with rotation. This ink penetrates into the alveoli of the cylinder being removed excess ink by a squeegee, thus the tile passes under the cylinder and the ink is transferred to the support.

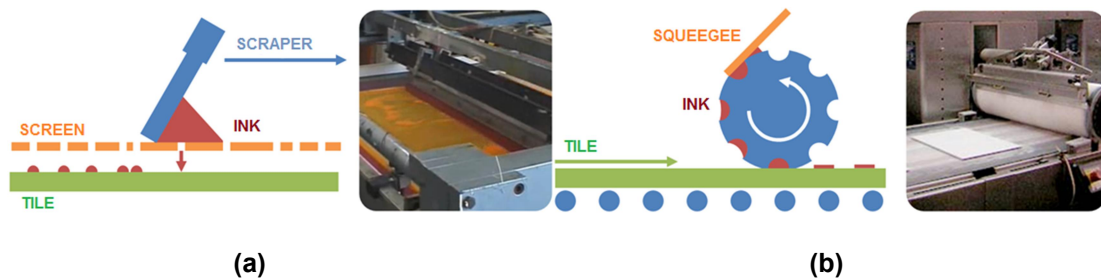


Figure 1-2. (a) System of ceramic decoration by screen printing and (b) by gravure

The main differences between digital inkjet and traditional processes are the following:

Table 1-1. Differences between traditional processes and digital inkjet³

| | Screen Printing/ Gravure (S/G) | Digital Inkjet (DI) | Best |
|------------------------------|--------------------------------|-----------------------------|------|
| Process | Contact with tile | Non-contact with tile | DI |
| Tile breakage | Common | Minimized | DI |
| Graphic pattern | Repeated | Unlimited | DI |
| Edges | Unpainted | Painted | DI |
| Model change | Takes hours | Without stopping production | DI |
| Production batches | Long | Upon request | DI |
| Stock and consumables | Screens and / or rollers | Without hardware decoration | DI |
| Stock | 100-200 inks | Only 4 inks | DI |
| Tone settings | Long and costly | Easy | DI |
| Graphic design | Physical support | Digital support | DI |
| Ink range | Wide variety of colors | Limited colors | S/G |
| Inks price | 3-6 €/Kg | 20 €/Kg | S/G |
| Ink consumption | 25-40 gr/m ² | 5-8 gr/m ² | DI |
| Workforce | A lot | Little | DI |
| Inversion | Low | High | S/G |
| Relief decoration | Limited | Unlimited | DI |
| Ink PSD | 1-15 µm | 0.1-0.5 µm | S/G |

Digital inkjet is the printing technique that more advantages offers such as it can be observed in *Table 1-1* although it also presents some disadvantages which are difficult to solve.

Nowadays the tile decoration is performed by digital inkjet due to advantages that offers. *Figure 1-3* shows the conversion rate from traditional to digital inkjet processes in 2014.⁴

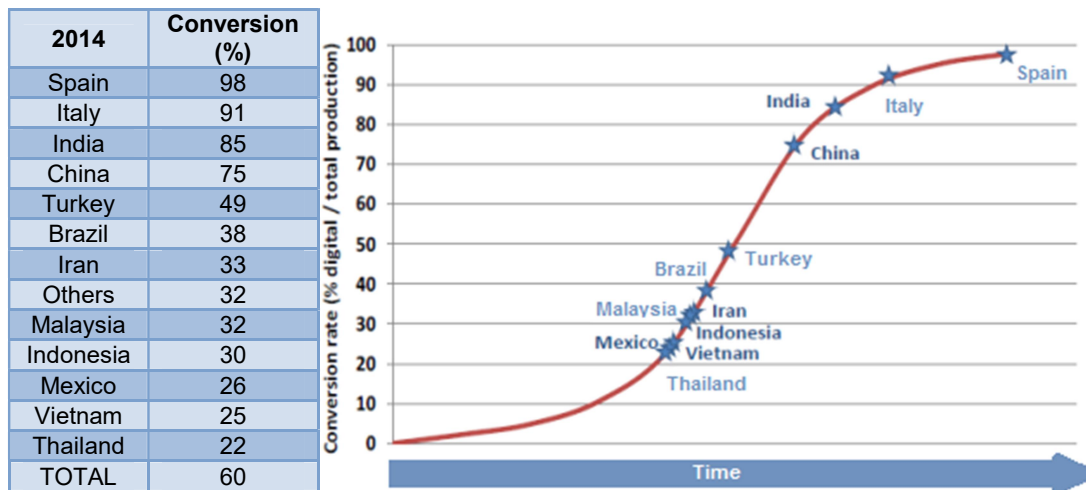


Figure 1-3. Conversion rate from traditional to digital inkjet processes by countries in 2014

The number of digital inkjet machine installed in the world has been 8800, which suppose a 60% of conversion rate about traditional processes. Implementation of this technology has not homogeneous. Conversion process has been led by Spain with a conversion rate of 98% (inkjet machine fabrication, application to tile production and bet by ink manufacturers).

Digital inkjet technology

The **printhead** is the section of an inkjet printing system that generally contains multiple nozzles for the jetting of ink onto the substrate (any surface to be printed on) to create an image. An ink supply system including an ink reservoir is generally attached by a hose.^{5, 6}

There are two main types of inkjet printing technologies because each is best suited to certain tasks:

- Continuous inkjet (CIJ)

This technology is a system where there is a continuous flow of ink from a pressurized reservoir. Acoustic or ultrasonic pressure waves break the stream of ink into individual droplets, which are then variably charged by passing through an electric field. The strength of the charge on the drop determines how far the droplet deflects and where the drop will land on the substrate. These deflected droplets build up the image and the non-charged droplets are collect in a gutter and recirculated.⁷

- Drop-on-demand or impulse inkjet (DOD)

This technology means that a drop of ink is only generated when it is needed, so ink waste is minimized. Within DOD inkjet printing, there are two main types of technologies: thermal and piezoelectric. Piezoelectric printheads use a ceramic material that undergoes distortion when an electric field is applied (the reverse piezoelectric effect), and this distortion is used to mechanically create a pressure pulse that causes a drop to be ejected from the nozzle.⁸⁻¹⁰

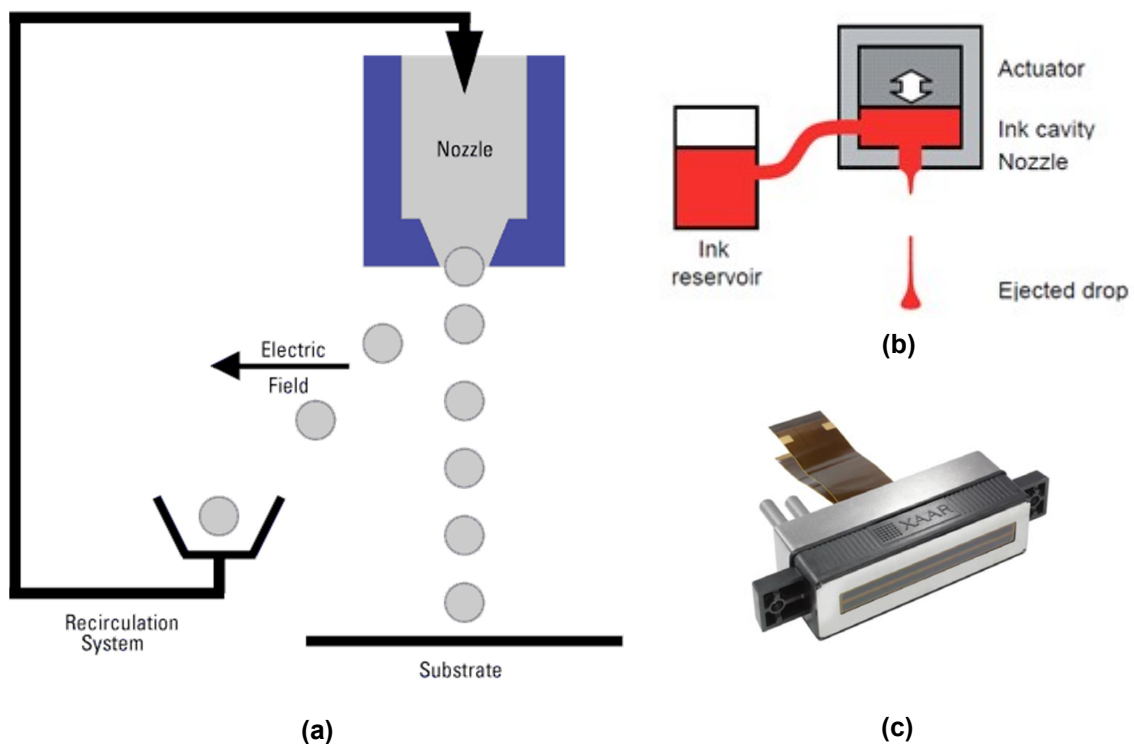


Figure 1-4. (a) Schematic illustration of continuous inkjet printing, (b) Schematic illustration of DOD inkjet printing and (c) Illustration of a Xaar printhead

In order to achieve specific printing applications, the whole printing system should be evaluated, namely the *printhead*, the fluid that is jetted from the printhead (*inkjet ink*), and the *substrate* onto which the ejected droplets are placed. For each application, the requirements are established, defining type of fluid chemistry, which directs the selection of the hardware and drives the implementation.

Digital inkjet use **DOD technology** and **piezoelectric printheads** in decoration printers in ceramics industry.

The use of inkjet inks in ceramic tile printers involves a range of requirements to be followed:

- Its composition must be compatible with the printing equipment (printer, printheads and pumping systems), avoiding possible interactions and degradations.
- Low evaporation speed in order to minimizing and preventing drying of the ink inside the printhead that causes nozzle clogging. Evaporation causes an increase in viscosity and thus particle agglomeration.
- Stability of the ink inside the printhead avoiding alterations in their physical and chemical properties due to sedimentation. In order to avoid it, ceramic tile printers and printheads have ink recirculation systems.
- Thermal stability of the ink preventing its degradation to the working temperatures of the printhead. This can cause changes in the chemical properties and physical both inks.
- Wettability of the ink avoiding drying in the print nozzles and favoring the wetting of the printhead.
- Facilitate filtering the ink through small holes and in this way favoring the passage therethrough and preventing abrasion thereof. In addition, ceramic tile printers have a filter which removes large particles in order to avoid the blockage of printheads.
- Present suitable physicochemical properties for printing systems (such as viscosity, surface tension, particle size distribution, etc.).

The physicochemical properties of inkjet inks are established by the printhead used. Piezoelectric printhead requires the following properties:

Table 1-2. Properties required by piezoelectric printhead

| Ink properties | Typical values |
|--|-----------------|
| Density (g/cm ³) | 1,35-1,50 |
| Viscosity at 25 °C (cP) | 20-30 |
| Surface tension (mN/m) | 25-35 |
| Particle size distribution, d ₉₀ (nm) | < 500 |
| Stability (height of sediment) | <0,5 mm in 24 h |

Inkjet inks composition

An inkjet ink is constituted mainly by:

- 1) **Solids** (30-50% weight): Inorganic pigments, frits or raw material of ceramic nature.
- 2) **Carriers**: Polar solvents (glycols, alcohols and water-based) and apolar solvents (fatty acid, esters and paraffins).
- 3) **Additives** (5-10% weight): Dispersants, humectants, rheology modifiers, surfactants, defoamers...

This components form a disperse system where the carrier is the disperse medium and pigment particles are the disperse phase. The additives such as dispersants provide colloidal stability to the disperse system.

- 1) Depending on the type of solid which constitutes the ink, there are two main types of ceramic inks:

- **Pigmented inkjet inks**, where the solid which constitutes the ink is an inorganic pigment.

Ceramic inkjet colors such as blue, brown, pink, yellow, red brown, black, beige and green, together they provide a wide color space, very appropriate for ceramics.

- **Unpigmented inkjet inks** (called effect inks, too); when solid is a frit or a raw material of ceramic nature.

Effects such as white, reactive, gloss, brightness, matt and metallic allow texture, gloss, opacity and some special effects to be obtained.



Figure 1-5. (a) Ceramic inkjet colors and (b) Effects

- 2) A carrier is a solvent through which pigment particles are dispersed. It is used as a transport of pigment particles since the ink reservoir until the ceramic tiles. Finally, carrier is evaporated totally in the step of kiln cure of tile.

Some characteristics that carrier should accomplish are viscosity, odorless, green solvent, water and printer compatibility and low volatility.

- 3) There are many types of additives, the followings are the main:

Humectants: Improve the wetting of the pigment particles by the carrier.

Surfactants: Modify the surface tension of the ink.

Defoamers: Destroy bubbles and foam which is formed in the ink.

Rheology modifiers: Reduce the tendency to sedimentation of the ink because increase viscosity.

Dispersants: Facilitate the dispersion of the pigment particles in the carrier, avoiding particle agglomeration and destabilization phenomena. They are due to the inherent stability of most dispersion systems.

The effects of the dispersant that takes place in a suspension are the followings:

- Improve the **wetting** between the pigment particles and the carrier. It is due to dispersant has a certain interaction with the surface of the pigment particles (adsorption) and with the carrier (solvation).
- Maintaining the pigment particles fully integrated into the carrier in order to improve **grinding** efficiency.
- Producing a **stabilization** of the pigment particles to prevent the formation of aggregates of particles.

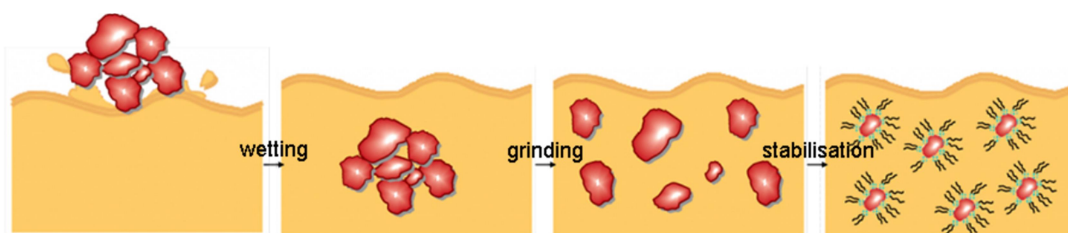


Figure 1-6. The different effects of a dispersant in a suspension

There are two types of stabilization:

- **Steric stabilization**

In a disperse system with pigment particles and solvent, there are interactions due to van der Waals forces which take place when particles approach each other and a minimum energy is reached, as shown in *Figure 1-7 (a)*. Aggregate of particles causes a reduction of gloss and intensity of color in a ink.

In order to achieve a stable dispersion of pigment particles, it is necessary to evaluate different dispersants and find their optimal concentration.

The dispersant concentration is of great importance. There is an optimal concentration of dispersant that can be determined by size and viscosity measurements. It can be observed in *Figure 1-7 (b)* that the viscosity of the dispersion usually decreases with the increase in dispersant concentration, up to a certain concentration, followed by increasing viscosity above that concentration.

The dispersant chosen should have anchoring groups enabling its adsorption on the pigment surface and have stabilizing groups enabling fragments of the dispersant to be extended into the solution.

When pigment particles stabilized with dispersant try to approach each other due to van de Walls forces, the stabilizing groups of dispersant begin to overlap and repulsion is caused between particles. Curve of repulsion due to suitable dispersant is shown in *Figure 1-7 (a)* and steric stabilization is provided by dispersant, as shown in *Figure 1-8 (a)*.

The result energy (total energy) of the sum between the attraction of van der Waals forces and the repulsion of steric stabilization can be observed in *Figure 1-7 (a)*.¹¹

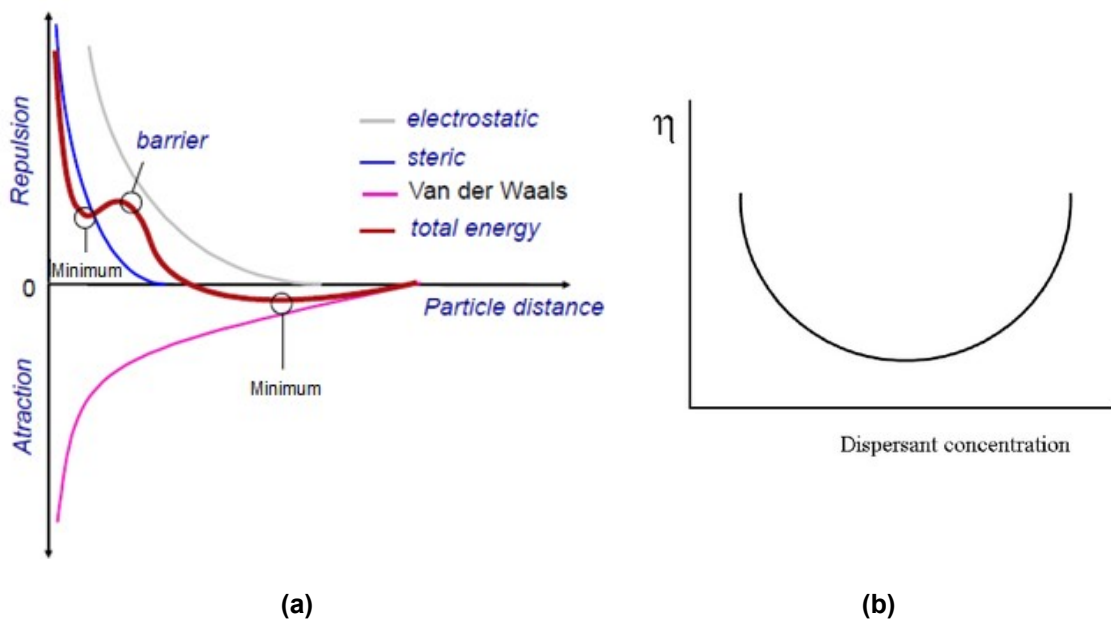


Figure 1-7. (a) Total interaction energy curves of a colloidal system and (b) Typical dependence of dispersant concentration on ink viscosity

- Electrostatic stabilization

The particles suspended in water usually have a surface charge. A cloud of counterions will be accumulated around this surface charge to offset this charge. The surface charge and the cloud of counterions form an electrical double layer. When two particles approach, electrical double layer of each particle begins to overlap and repulsion is caused between particles (*Figure 1-8 (b)*), the attraction by van der Waals between particles is counteracted and dispersion is stabilized. All curves of energy can be observed in *Figure 1-7 (a)*.

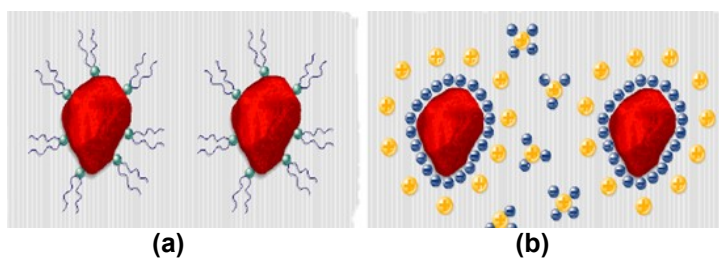


Figure 1-8. (a) Steric stabilization and (b) Electrostatic stabilization

Main properties of inkjet inks

The inkjet inks should meet specific physicochemical properties, which depend on its intended use, and all of them should remain constant over a prolonged period of time. This one is known as “*shelf life*” and it is typically two years storage at room temperature. The main ink parameters that they have been considered while preparing the ink are discussed below.

STABILITY

Inkjet inks are suspensions formed by liquid (disperse medium) and solid (disperse phase) as it stated above. Their stability or instability can be determined according to the destabilization phenomena that occur in these.

A stable suspension will be that which keeps constant its properties over time. Instead, suspension will be unstable if it has change in its properties. Dispersions are unstable from the thermodynamic point of view; however, they can be kinetically stable over a large period of time.

Destabilization phenomena of dispersion can be classified into two processes:

- **Particle size increase phenomena** (flocculation or coalescence).
- **Migration phenomena** or phase separation (creaming or sedimentation).

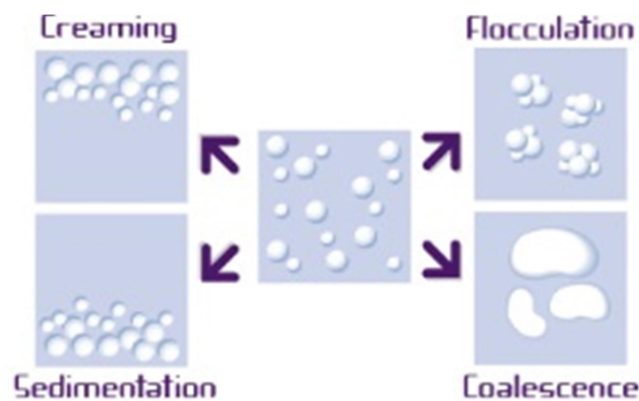


Figure 1-9. Destabilization phenomena of a dispersion

Creaming is a common phenomenon of instability for suspensions that lead to a phase separation. It is due to the dispersed phase has a lower density than the continuous phase; it will finally lead to a phase separation.

Sedimentation is a phenomenon similar to the previous one and it leads to a phase separation, too. It occurs when the density of the dispersed phase is greater than the density of the continuous phase.

Coalescence and flocculation phenomena are physic-chemically very different but they both lead to an increase in the size of the particles. **Coalescence** is an irreversible process which leads to the fusion of the interfaces, hence the creation of one single drop. On the other hand, the **flocculation** is only an aggregation of the particles and if it is irreversible, it is called coagulation.¹²

Creaming or sedimentation can be coupled with coalescence or flocculation and will finally lead to a phase separation.

Stability is an important property because if there is sedimentation, other properties are altered such as viscosity which increases due to flocculation or coalescence of particles. In addition, it is necessary that there is the minimum amount of sediment in the ink because the ink is easier of recover through stirring.

RHEOLOGICAL BEHAVIOR

Rheological behavior of an ink is measured by viscosity and pseudoplasticity index.

Depending on the flow behavior acquired when a shear stress or shear rate is applied, there are different behaviors which can be observed below (Figure 1-10 and 1-11):

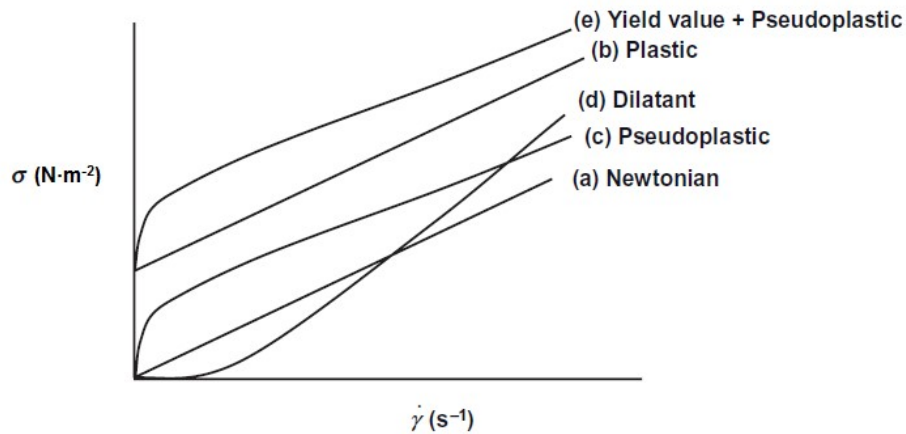


Figure 1-10. Flow curves for various systems

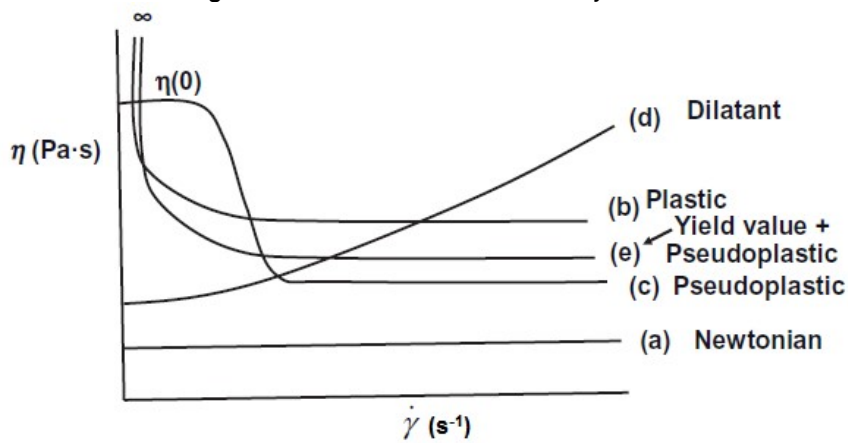


Figure 1-11. Viscosity - shear rate relationship

Although there are a lot of flow behaviors, only those which appear in this project will be explained.

Newtonian Systems (Newton's Law of viscosity)

The resistance that appears from the lack of slipperiness of parts of a liquid is proportional to the velocity with which the parts of the liquid are separated one from another. The shear rate is a single valued function of the shear stress (*Figure 1-12*), i.e., the shear stress ($\text{N}\cdot\text{m}^{-2}$) versus shear rate (s^{-1}) is linear, and the slope is equal to the *dynamic viscosity*, η ($\text{Pa}\cdot\text{s}$):

$$\sigma = \eta \dot{\gamma} \quad (1.1)$$

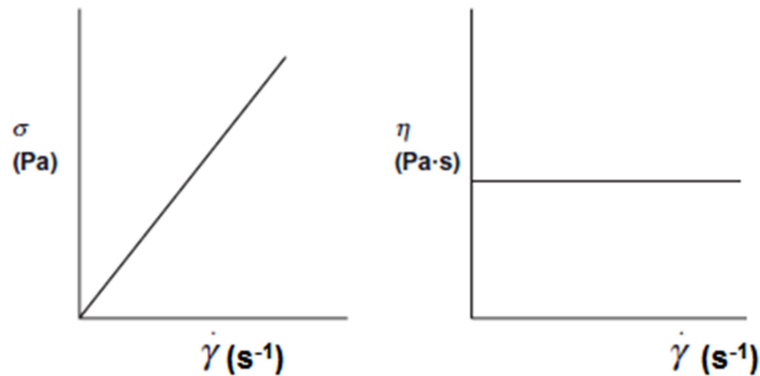


Figure 1-12. Newton's law

Non - Newtonian Systems: Pseudoplastic System

The materials which fit this type of model are usually formed by elongated particles (anisotropic). This one is fundamental to explain the behavior of these fluids. Particles intersect with each other opposing movement at rest and when the liquid begins to flow are going untangling and guiding in the direction of flow. These materials need a minimum shear rate or shear stress to begin to flow. Process is reversible; when shear rate or shear stress is stopped they begin to interbreed again.

This system shows a limiting viscosity $\eta(0)$ at low shear rates (this is referred to as "residual" or "zero shear" viscosity). The flow curve can be fitted to a power law fluid model:

$$\sigma = k \dot{\gamma}^n \quad (1.2)$$

Where k is the consistency index and n is the shear thinning index ($n < 1$).¹³

The viscosity is of great importance for ink performance during jetting through printhead at 40°C and spreading on the substrate. It is affected by several parameters (the presence and concentration of polymeric additives, surfactants, solvent composition and flocculation...). Most current inkjet inks have a constant viscosity over a wide range of shear rates, i.e., they are Newtonian. Therefore the pseudoplasticity index value in an ink is searched as small as possible. Its viscosity is very low and it depends on printhead that the inkjet ink will be used. A viscosity value close to 20 cP is usually uses in piezoelectric printhead.¹⁴

Before it has been said that the viscosity is affected by stability but stability is influenced by viscosity, too. A low viscosity of the ink provides a bad stability of the ink and the apparition of sedimentation phenomena.

SURFACE TENSION

The surface tension of the ink is a primary factor determining droplet formation and spreading on the substrate upon contact. It can be controlled through:

- **Surfactant.** This one is usually used at very low concentrations (below of 1 or 0.1% w/w). It means that even a slight change in the surfactant concentration may cause a significant change in the ink performance. When surface tension is controlled by surfactant, the dynamic surface tension should be considered.
- **Suitable solvent compositions (Carrier).** When surface tension results from the composition of the liquid medium, it will not change over time. The surface tension value will be that of equilibrium conditions, which can be readily measured by conventional methods, such as the DuNoüy ring or Wilhelmy plate method (static surface tension).¹⁵

Surface tension can be measured in two ways:

- **Static measurements.** They are determined for a surface that is assumed to be at equilibrium.
- **Dynamic measurements.** They are made on systems that are assumed to not be at equilibrium.

Table 1-3 shows the different methods which allow measure the surface tension:

Table 1-3. Types of surface tension measurements

| Surface Tension Measurements | |
|------------------------------|-------------------------|
| Equilibrium methods | Dynamic methods |
| Ring (DuNoüy) | Maximum Bubble Pressure |
| Plate (Wilhelmy) | Oscillating Jet |
| Capillary Rise | Drop Volume (or weight) |
| Pendant Drop | Surface Waves |
| Sessile Drop | |
| Spinning Drop | |

DENSITY

Density is one of the parameters which determining droplet formation.

PARTICLE SIZE DISTRIBUTION

If the particle size is too large can cause a blockage in the filter of ceramic tile printers and stability problems due to the tendency to settle.

On the contrary, if the particle size is too small due to excessive grinding, the pigment may lose some of their color.

2. OBJETIVES

Nowadays digital inkjet technology is extended in the ceramic industry as mentioned in the introduction. The majority of the research in this sector is focused on the development of both pigmented and non-pigmented (effect inks) inkjet inks.

Therefore, the main objective of this work is the development of several formulations of effect inks.

General Objectives

- The study of the properties which an inkjet ink must have.
- The study of several formulations of effect inks.
- Learning the basis of the techniques to characterize the inkjet inks.
- Learning how to perform a design of experiments by ECHIP.

Specific Objectives

- The performing of design of experiments.
- The formulation of different compositions of a system with alumina.
- Learning to use a ball mill in laboratory scale.
- The evaluation of the following properties: Particle size distribution, rheological behavior, stability against sedimentation, surface tension and density.
- The study the effect of different variables suggested in experimental design.
- Get the optimum composition.
- Comparing the properties of the optimum composition with the expected.

3. EXPERIMENTAL SECTION

3.1. Experimental Design

The basic idea of experimental design is to discover the relationship between a response and one or more control variables. If y is a response, say viscosity of a ink, and x_1, x_2, \dots, x_n are a set of control variables, say percentage of dispersant, percentage of solid content, etc., then it is possible to suppose a functional relationship between the response and the control variables, like:

$$y = f(x_1, x_2, \dots, x_n) \quad (3.1)$$

Using this equation, the intention is to better understand the process but the form of this equation is not known in the majority of cases. It can be approximated to a polynomial function such as a linear or quadratic function and then it can be used to predict values of y , for new combinations of the control variables.

First of all, it is necessary to define the components of the ink. Then, design variables, its variation intervals, its possible restrictions and its properties which will be optimized are defined.

The control variables and its variation intervals are introduced in program of experimental design together with the components of the ink. A mathematical model is defined and the design is executed. Experimental design provides a table with all combinations of components of ink (compositions).

Next, all compositions are prepared and characterized in order to determine the properties defined previously. Once all compositions are characterized; the value of the properties is introduced in the experimental design and a mathematical adjustment is performed. Later, results interpretation and the study of effect of control variable on the properties are performed. In this way, it is possible to know the relationship between the response and the control variables and it is possible to carry out an optimization.

This one consists of establish a range of conditions or desired properties and experimental design calculates the combination of control variables necessary to achieve this expected properties through the *Equation (3.1)*. Finally, optimal composition is characterized.

In this experimental design it was used ECHIP software, which allows establish the different compositions of a suspension that are characterized, analyze the results statistically and do the optimization by an easy form.^{16, 17}

3.2. Components of Ink

First of all, it was necessary to specify the system which would be studied. It was an unpigmented inkjet ink which was constituted by:

1) Solid: A raw material of ceramic nature, *alumina*.

MARTOXID® MR70 was provided by Albemarle Corporation and it is raw material of ceramic nature. Its composition and characteristics can be seen in the *Table 3-1*.

Table 3-1. Composition and characteristics of MARTOXID® MR70

| | | |
|--|------------|---|
| Al₂O₃ | [%] | ≈ 99.8 |
| Na ₂ O total | | ≤ 0.1 |
| CaO | | ≈ 0.02 |
| Fe ₂ O ₃ | | ≈ 0.02 |
| SiO ₂ | | ≈ 0.08 |
| MgO | | ≈ 0.06 |
| α-Al₂O₃ | [%] | ≥ 95 |
| Particle Size Distribution (Cilas 1064) | [μm] | d ₁₀ = 0.1 – 0.4 d ₅₀ = 0.5 – 0.8 d ₉₀ = 1.5 – 3.0 |

2) Carrier: An apolar solvent, ester type of fatty acid, *Printojet C-28*.

PRINTOJET C-28 is a natural solvent based on ester which is derivate of fatty acids and it was provided from Lamberti. Its polarity is low and it confers to ink a low viscosity, a good “shelf life” and an important resistance to sedimentation and aggregation. It is used to mill inorganic pigments in systems of micrometers scale in formulations of inks for different inkjet applications.

Table 3-2. Physicochemical characteristics of Printojet

| | |
|--|------------------------------|
| Aspect at 20 °C | Transparent yellowish liquid |
| Viscosity (Haake rheometer, 100 s ⁻¹ , 25 °C) | 8 – 9 cP |
| Density (g/L) at 25 °C | 865 |

3) Additives: A dispersant additive, *UBEDISP1b65-N2*.

UBEDISP1b65-N2 is a dispersant additive provided by UBE Corporation Europe.

3.3. Control Variables and Compositions

Once the system was set out, it was necessary to define the control variables, their intervals of variation and the properties (responses) to be optimized.

The following two continuous variables and their intervals of variation were defined:

- % Additive: 2 – 5 %
- % Content in solids: 30 – 40 %

Furthermore, a discrete variable was defined:

- Time of milling: 60 or 90 minutes

The mentioned variables were introduced in the ECHIP software and **lineal design with a central point** was executed. The combination of the different variables was obtained by the program. There was a composition for each combination and they were shown in the *Table 3-3*.

Table 3-3. Compositions obtained by ECHIP

| Composition | Components | | | Time of milling (min) |
|-------------|------------|-------------|------------------|-----------------------|
| | % Alumina | % Printojet | % UBEDISP1b65-N2 | |
| 1 | 40 | 55 | 5 | 90 |
| 1' | 40 | 55 | 5 | 90 |
| 2 | 30 | 68 | 2 | 60 |
| 3 | 30 | 65 | 5 | 60 |
| 4 | 40 | 58 | 2 | 90 |
| 5 | 40 | 58 | 2 | 60 |
| 6 | 30 | 65 | 5 | 90 |
| 7 | 30 | 68 | 2 | 90 |
| 8 | 40 | 55 | 5 | 60 |
| 9 | 35 | 61.5 | 3.5 | 60 |
| 10 | 35 | 61.5 | 3.5 | 90 |

**Compositions 1 and 1' was the same, but comma was introduced in order to distinguish two compositions 1 when it was necessary.*

3.4. Preparation of Compositions of Unpigmented Inks

The following phases were used to prepare the different compositions of unpigmented inks:

Step 1. Preparation of compositions

The unpigmented inks were prepared according to the different compositions which were proposed by the ECHIP.

First, organic carrier (Printojet) was introduced into a glass beaker. Then, dispersant was added and mixed with vigorously agitation. Finally, alumina was put in beaker and all components were blended with vigorously agitation, too.

Quantities used (*Table 3-4*) of carrier, dispersant and alumina were referred to a total of 1000 g according to the percentages of the compositions of *Table 3-3*.

Table 3-4. Quantities used in the composition

| Composition | Components | | |
|-------------|-------------|-------------|--------------------|
| | Alumina (g) | Vehicle (g) | UBEDISP1b65-N2 (g) |
| 1 | 400 | 550 | 50 |
| 1' | 400 | 550 | 50 |
| 2 | 300 | 680 | 20 |
| 3 | 300 | 650 | 50 |
| 4 | 400 | 580 | 20 |
| 5 | 400 | 580 | 20 |
| 6 | 300 | 650 | 50 |
| 7 | 300 | 680 | 20 |
| 8 | 400 | 550 | 50 |
| 9 | 350 | 615 | 35 |
| 10 | 350 | 615 | 35 |

Really, not all compositions were prepared and the reason is explained then.

Once all compositions were prepared, the following phase is the grinding in a mill. As it has seen before, one variable was the time of milling (60 or 90 minutes) and it is possible to see in the *Table 3-3* that there are two identical compositions for each time of milling. In order to carry out the millings more quickly, only one composition was prepared for each two times of grinding. So, different compositions were prepared and they were introduced in the mill, later, a sample of ink was taken at 60 minutes and then the rest of ink was taken at 90 minutes. The quantity of the samples which were taken at 60 minutes was the necessary to make the different analysis of characterization (50 ml).

Therefore, only the next compositions which can be seen in *Table 3-5* were prepared:

Table 3-5. *Compositions prepared really*

| Composition | Components | | |
|-------------|-------------|-------------|--------------------|
| | Alumina (g) | Vehicle (g) | UBEDISP1b65-N2 (g) |
| 1, 8 | 400 | 550 | 50 |
| 1' | 400 | 550 | 50 |
| 2, 7 | 300 | 680 | 20 |
| 3, 6 | 300 | 650 | 50 |
| 4, 5 | 400 | 580 | 20 |
| 9, 10 | 350 | 615 | 35 |

**The composition 1 was performed two times to check the experimental error.*

Step 2. Grinding of compositions

Once all compositions were prepared, the charges of grinding were prepared with them and they were introduced into LABSTAR mill of microballs of Netzsch (*Figure 3-1*). The objectives of milling are the reducing the particle size to achieve a particle size distribution lower than 0.5 μm and the reaching of an intimate mixture of the alumina particles with the dispersant.



Figure 3-1. *LABSTAR mill of microballs of Netzsch*

The conditions of milling which were used are below:

- Mill chamber of 1 L. A total of 1000 g of suspensions were prepared due to the capacity of the chamber that was used.
- Milling was made with a rotor velocity of 3600 rpm. The mill was connected to a refrigeration system during all the process in order to the temperature of suspension was not higher of 50 °C.
- Velocity of turn of rotor was constant for each milling time.
- Elements of milling used were ZETABEADS® of 0.3 mm; their characteristics are detailed in the following *Table 3-6*.

Table 3-6. Physicochemical characteristics of the balls used for milling

| Chemical composition about (in weight %) | | Mechanical properties | |
|--|----|-----------------------|-----------|
| ZrO ₂ + HfO ₂ | 95 | Density | 6.0 kg/l |
| Y ₂ O ₃ | 5 | Bulk density | 3.6 kg/l |
| | | Young modulus | > 200 GPa |
| | | Vickers hardness | > 1200 HV |

Before of the milling, a pre-grinding was done because particle size distribution of alumina was too big ($d_{90} = 1.5 - 3.0 \mu\text{m}$). Time of pre-grinding was 120 minutes with ZETABEADS® of 0.8 mm and it was performed on all suspensions. Then, milling was applied.

Step 3. Characterization of the suspensions

The compositions were characterized after milling to determine the following physical properties:

- **Particle size distribution:** d_{10} , d_{50} , d_{90} were determined by a MASTERSIZER 2000 laser diffraction equipment of MALVERN (*Supplementary material 1*).
- **Rheological behavior:** viscosity and pseudoplasticity index were calculated with a CVO-120 HR BOHLIN rheometer (*Supplementary material 2*).
- **Stability against sedimentation:** ΔBS (%) at 8 h, ΔBS (%) at 24 h, sediment height (mm) and start sedimentation (h) were identified by an optical scanning analyzer, Turbiscan Lab Expert of FORMULACTION (*Supplementary material 3*).
- **Surface tension** was determined using a tensiometer of Krüss, model K12. (*Supplementary material 4*).
- **Density** was determined with a pycnometer. (*Supplementary material 5*).

4. RESULTS AND DISCUSSION

4.1. Results

Characterization of compositions is not only the most important thing in an experimental design. Moreover, it is necessary to perform of mathematic adjust that shows the relationship between the properties resulting and the design variables and results are interpreted in order to predict properties for the remaining variables combination. In this manner, it is possible to formulate the compositions that more adjust to the established criterion.

Compositions of suspension proposed by ECHIP were characterized and the following results were obtained for the different properties (*Table 4-1 to 4-4*):

Table 4-1. Particle Size Distribution

| Composition | d ₁₀ (µm) | d ₅₀ (µm) | d ₉₀ (µm) |
|-------------|----------------------|----------------------|----------------------|
| 1 | 0.153 | 0.255 | 0.406 |
| 1' | 0.156 | 0.261 | 0.420 |
| 2 | 0.148 | 0.247 | 0.399 |
| 3 | 0.156 | 0.260 | 0.417 |
| 4 | 0.148 | 0.246 | 0.393 |
| 5 | 0.141 | 0.228 | 0.361 |
| 6 | 0.146 | 0.240 | 0.385 |
| 7 | 0.145 | 0.240 | 0.385 |
| 8 | 0.155 | 0.262 | 0.423 |
| 9 | 0.151 | 0.253 | 0.406 |
| 10 | 0.141 | 0.231 | 0.372 |

Table 4-2. Rheological Behavior

| Composition | Viscosity (cP) | Pseudoplasticity Index (cP) |
|-------------|----------------|-----------------------------|
| 1 | 24.411 | 0.749 |
| 1' | 25.028 | 0.897 |
| 2 | 16.166 | 0.339 |
| 3 | 20.962 | 0.513 |
| 4 | 21.112 | 0.567 |
| 5 | 20.556 | 0.588 |
| 6 | 21.198 | 0.514 |
| 7 | 16.384 | 0.319 |
| 8 | 24.025 | 0.790 |
| 9 | 18.870 | 0.434 |
| 10 | 19.010 | 0.430 |

A lower pseudoplasticity index involves a higher Newtonian behavior because this index is calculated from two viscosities which are measured at different shear rate (Supplementary material 2).

Table 4-3. Stability against sedimentation

| Composition | Δ BS (%) 8h | Δ BS (%) 24h | h (mm) at 24h | Start sedimentation (h) |
|-------------|-----------------------|------------------------|------------------|----------------------------|
| 1 | 1.7 | 4.5 | 0.6 | 5.5 |
| 1' | 1.3 | 3.4 | 0.6 | 4.5 |
| 2 | 6.7 | 7.7 | 0.2 | 1.0 |
| 3 | 3.9 | 5.4 | 0.5 | 2.5 |
| 4 | 3.3 | 7.3 | 0.7 | 2.5 |
| 5 | 6.8 | 8.1 | 0.3 | 1.5 |
| 6 | 1.2 | 3.1 | 0.6 | 7.0 |
| 7 | 3.2 | 6.7 | 0.7 | 2.5 |
| 8 | 5.1 | 6.6 | 0.5 | 2.5 |
| 9 | 6.5 | 7.8 | 0.3 | 1.5 |
| 10 | 2.8 | 6.2 | 0.7 | 4.0 |

Parameters calculated from Turbiscan affect to stability of the following manner:

- A higher Δ BS (%) 8h or 24h in the middle of sample implicates a lower stability.
- A higher h (mm) at 24h involves that there is more sediment after 24h, whereby suspension is more unstable when quantity of sediment is higher.
- Start sedimentation (h) indicates when the minimum quantity of sediment, which is possible to measure, appears. Hence a lower value for start sedimentation means that suspension is more stable because sediment takes more time in appear.

Table 4-4. Surface tension and density

| Composition | Surface Tension (mN/m) | Density (g/ml) |
|-------------|------------------------|----------------|
| 1 | 29.57 | 1.25 |
| 1' | 29.35 | 1.24 |
| 2 | 29.50 | 1.16 |
| 3 | 29.66 | 1.16 |
| 4 | 29.78 | 1.27 |
| 5 | 29.43 | 1.27 |
| 6 | 29.73 | 1.16 |
| 7 | 29.74 | 1.16 |
| 8 | 29.51 | 1.25 |
| 9 | 29.21 | 1.20 |
| 10 | 29.77 | 1.20 |

The following profiles (*Figures 4-1 and 4-2*) correspond to profiles obtained by Turbiscan for suspensions. Once all profiles were studied, they can be resumed in two different behaviors. One behavior belongs to compositions which were grinded during 90 minutes (*Figure 4-1*) and another behavior corresponds to compositions which were grinded during 60 minutes (*Figure 4-2*). In addition, destabilization phenomena such as sedimentation and flocculation or coalescence can be observed.

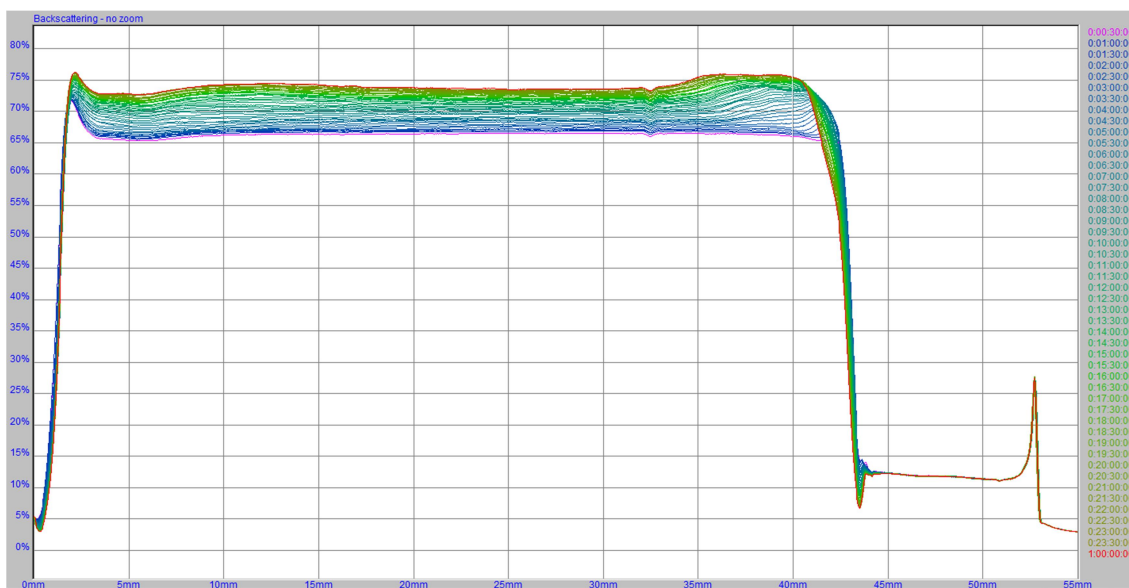


Figure 4-1. Profile obtained for suspensions milled at 90 minutes (composition 4)

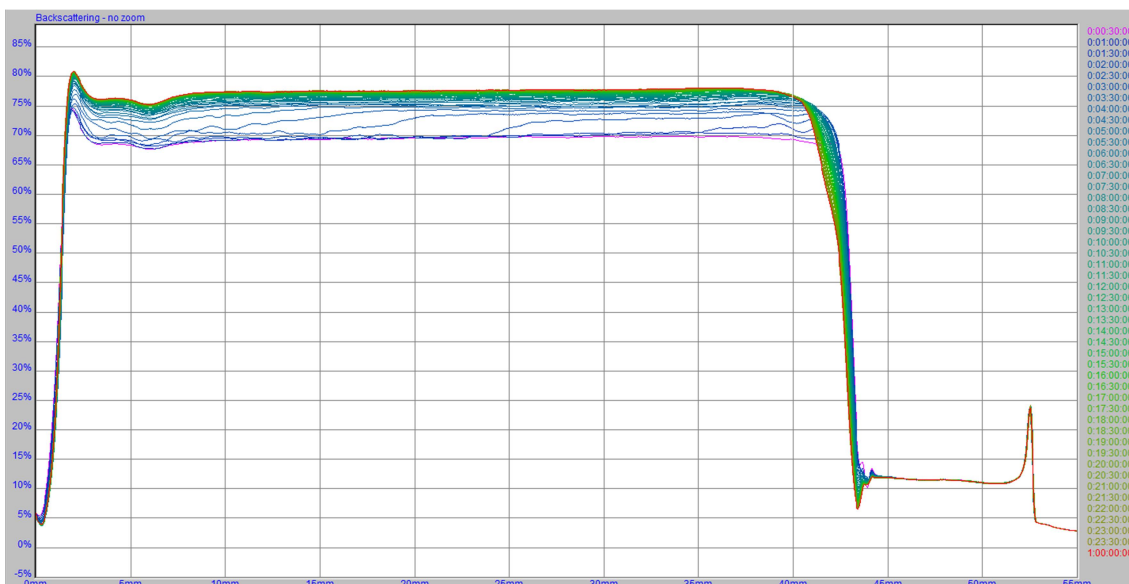


Figure 4-2. Profile obtained for suspensions milled at 60 minutes (composition 5)

If *Figure 4-1* and *4-2* are observed, it can be seen that the first profile obtained is displayed in pink, while the last one in red.

When sediment is appearing, the backscattering should be decreasing due to clarification front in the top of the cell. But, if *Figure 4-1* and *4-2* are observed, it can be seen that backscattering is increasing when sediment appears. It is due to:

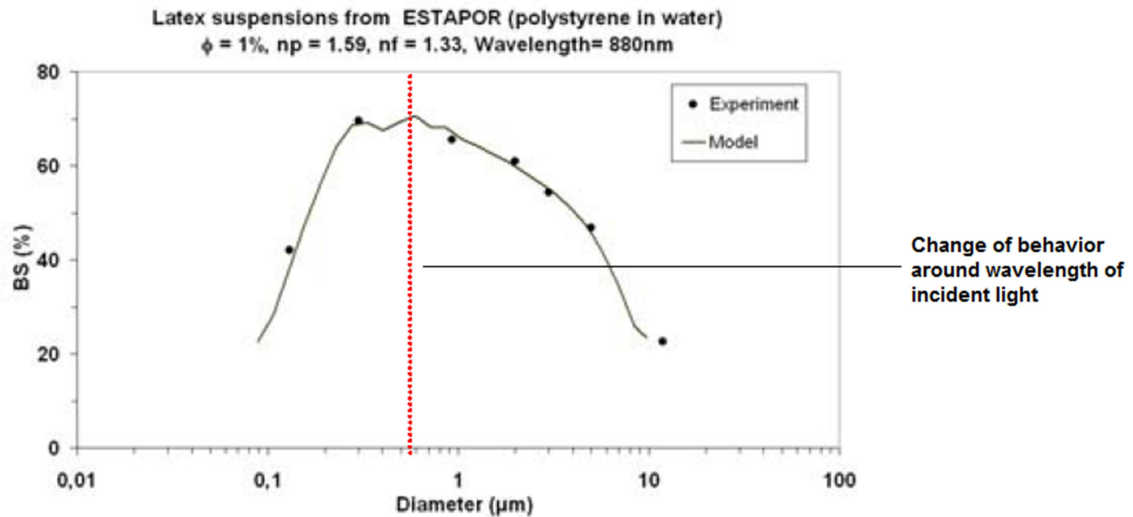


Figure 4-3. Evolution of the backscattering with the diameter of the particles

The variation of the backscattering level is shown in *Figure 4-3* as a function of the particle diameter for a fixed volume fraction of latex particles. The curve obtained is a bell shaped curve, where the top is linked to the wavelength of the incident light (880 nm).

Experimental values show that the backscattering increases with the particle mean diameter when the particles are smaller than the incident wavelength and it decreases with the mean diameter for particles larger than the incident wavelength.¹⁸

Hence, the backscattering is increased in this case because the particle mean diameter of pigment particles is lower than 880 nm.

4.2. Mathematical Model Adjustment and Interpretation of Results

All experimental results obtained were not introduced in the experimental design, only the following results:

- **Particle size distribution:** d_{90} .
- **Rheological Behavior:** viscosity and pseudoplasticity index.
- **Stability against sedimentation:** Δ BS (%) at 8h, Δ BS (%) at 24h, and start sedimentation (h).

These results (*Table 4-5*) were introduced in ECHIP and they were adjusted to a **lineal model**.

Table 4-5. Experimental results introduced in ECHIP

| Composition | Viscosity (cP) | Pseudoplasticity Index (cP) | d_{90} (μ m) | Δ BS (%) 24h | Δ BS (%) 8h | S_{sed} (h) |
|-------------|----------------|-----------------------------|---------------------|---------------------|--------------------|---------------|
| 1 | 24.411 | 0.749 | 0.406 | 4.5 | 1.7 | 5.5 |
| 1' | 25.028 | 0.897 | 0.420 | 3.4 | 1.3 | 4.5 |
| 2 | 16.166 | 0.339 | 0.339 | 7.7 | 6.7 | 1.0 |
| 3 | 20.962 | 0.513 | 0.417 | 5.4 | 3.9 | 2.5 |
| 4 | 21.112 | 0.567 | 0.393 | 7.3 | 3.3 | 2.5 |
| 5 | 20.556 | 0.588 | 0.361 | 8.1 | 6.8 | 1.5 |
| 6 | 21.198 | 0.514 | 0.385 | 3.1 | 1.2 | 7.0 |
| 7 | 16.384 | 0.319 | 0.385 | 6.7 | 3.2 | 2.5 |
| 8 | 24.025 | 0.790 | 0.423 | 6.6 | 5.1 | 2.5 |
| 9 | 18.870 | 0.434 | 0.406 | 7.8 | 6.5 | 1.5 |
| 10 | 19.010 | 0.430 | 0.372 | 6.2 | 2.8 | 4.0 |

Results were adjusted to a lineal model although adjust them to a lineal model with interactions was tried, too. The latter adjustment was not successful because interaction between alumina, vehicle and dispersant don't exist. This model would have been successful if it had been two dispersants or two vehicles.

Surface tension was not introduced in the program because it was very similar for all compositions (29.50 mN/m approximately). It is due to that surface tension depends on much of used carrier.

Density was not introduced in the software because only depends on solid content. Density is larger when solid content is greater.

Once results were introduced in ECHIP, it was possible to obtain the following information in order to interpret results obtained:

Qualitative influence of different variables

Preliminary influence of the different variable can be seen in the following table:

Table 4-6. Qualitative influence of variables in different properties

| | Viscosity | Pseudoplasticity Index | d ₉₀ | ΔBS (%) 24h | ΔBS (%) 8h | S _{sed} (h) |
|-----------------|-----------|------------------------|-----------------|-------------|------------|----------------------|
| % Dispersant | *** | ** | * | *** | *** | ** |
| % Solid content | *** | *** | | | | |
| Milling time | | | | ** | *** | ** |

Table 4-6 shows influence of variables qualitatively. Each asterisk indicates the importance of each variable, when more asterisks there are, this variable has more important in this property. Absence of asterisk shows that this variable has not importance in this property.

First conclusions can be observed in Table 4-6:

- The percentage of dispersant greatly affects the rheological behavior and stability against sedimentation.
- The percentage of dispersant greatly affects the rheological behavior.
- The milling time only greatly affects the stability against sedimentation.
- Particle size distribution (d₉₀) is not affected by any variables. It is due to the pre-grinding performed.

Quantitative influence of different variables

ECHIP provides numeric information of the influence of variables with the coefficients of the mathematic model terms. These coefficients are the following (Table 4-7):

Table 4-7. Coefficients of the mathematic model terms

| | Viscosity (cP) | Pseudoplasticity Index (cP) | d ₉₀ (μm) | ΔBS (%) 24h | ΔBS (%) 8h | S _{sed} (h) |
|-----------------|----------------|-----------------------------|----------------------|-------------|------------|----------------------|
| Constant | 20.313 | 0.535 | 0.389 | 6.2 | 4.1 | 3.0 |
| % Dispersant | 1.401 | 0.072 | 0.013 | -0.9 | -0.7 | 0.8 |
| % Solid content | 0.396 | 0.028 | 0.002 | 0.1 | - | - |
| Milling time | 0.197 | 0.003 | - | -0.9 | -1.7 | 1.2 |

From *Table 4-7* it is possible to obtain the form of the equation that shows the relationship between the response and the control variables.

An example would be the following:

$$\text{Viscosity (cP)} = 20.313 + 1.401 \cdot \% \text{ Dispersant} + 0.396 \cdot \% \text{ Solid content} + 0.197 \cdot \text{Milling time} \quad (4.1)$$

Where:

Viscosity is the response property;

% Dispersant, *% Solid content* and *milling time* are the control variables.

It can be observed in *Equation 4.1* that percentage of dispersant is more important than the percentage in solid content, because the coefficient of percentage of dispersant is greater. And it can be observed that coefficient of milling time is negligible.

The same equations could be written for the rest of the properties.

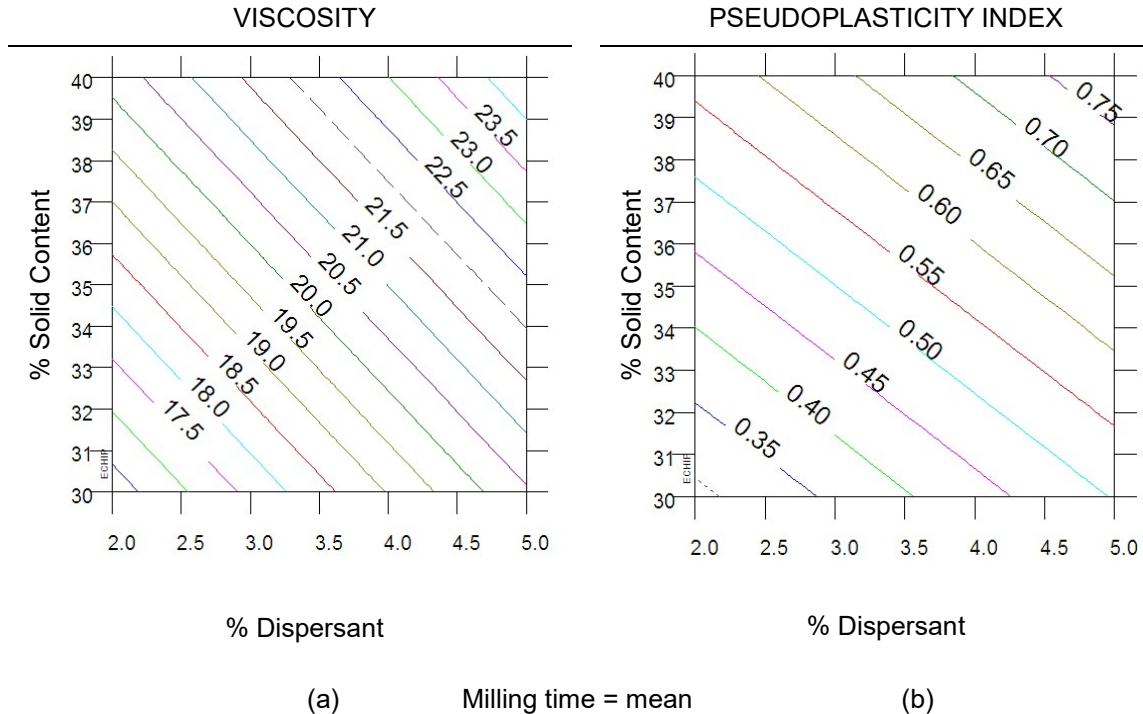
Trend graphs

Once lineal model was established, this software allows represent different graphs which connect the response properties and the control variables that were defined when the experimental design was defined.

Several 2D graphs were performed and lines of equality property were represented in them.

These graphs are better than the tables of results (*Table 4-1 to 4-4*) to interpret the results because graphs show better the trends than the tables. In this way, it is possible to know the relationship between response properties and control variables.

Viscosity and Pseudoplasticity Index

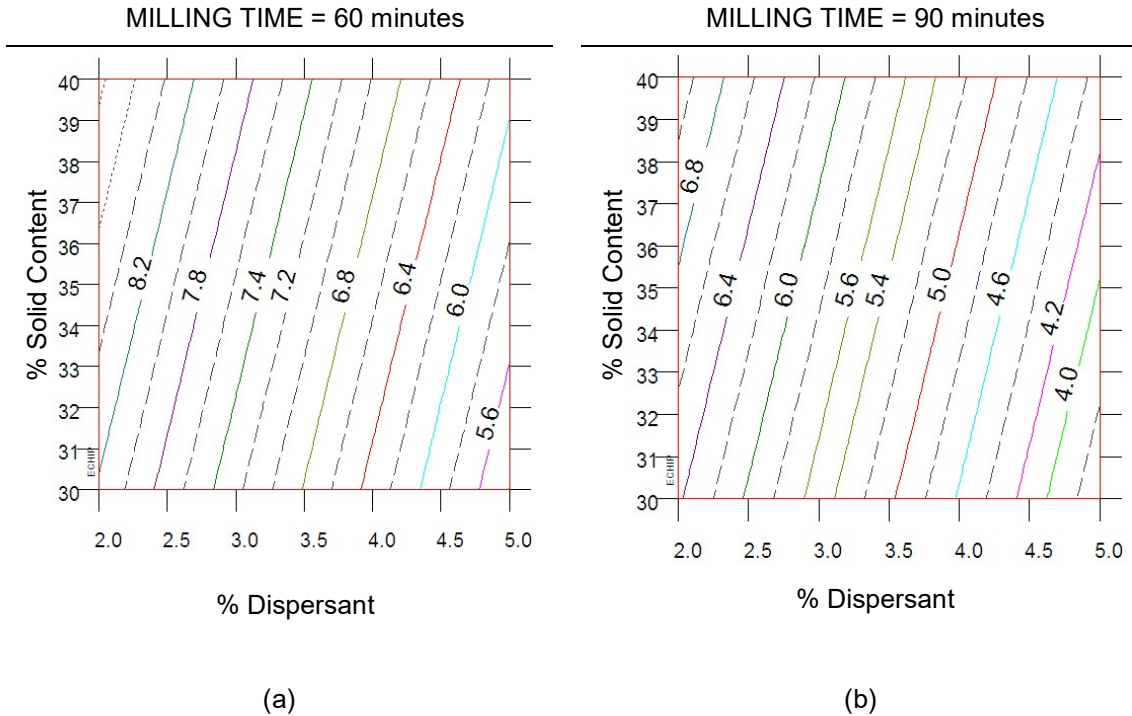


Graphic 4-1. (a) Viscosity tendency and (b) Pseudoplasticity index tendency

The following analysis was obtained from *Graphic 4-1*:

- Experimental design shows that compositions with higher viscosity values are those formulated with a bigger dispersant percentage and with a bigger solid content percentage.
- Experimental design suggests the same for the pseudoplasticity index. It is higher when compositions are formulated with a bigger dispersant percentage and with a bigger solid content percentage.
- The shape of lines of equality property indicates that the dependence of two properties is identical and its straight shape shows that there is not interaction between dispersant percentage and solid content percentage.
- Moreover, it can be observed that a higher viscosity always means a higher pseudoplasticity index.

Stability against sedimentation: Δ BS (%) 24h

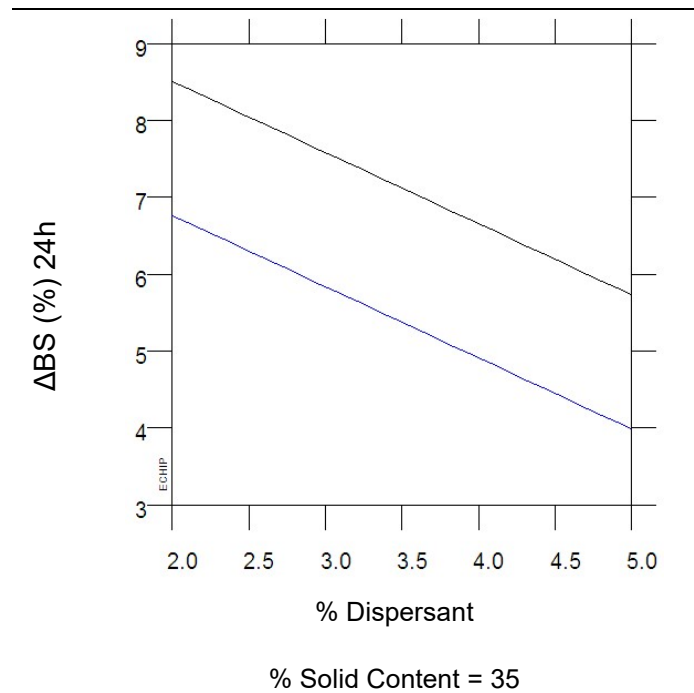


Graphic 4-2. (a) Δ BS (%) 24h tendency for 60 minutes of milling time and (b) Δ BS (%) 24h tendency for 90 minutes of milling time

It can be deduced from *Graphic 4-2*:

- Compositions which present higher stability against sedimentation are those formulated with a bigger dispersant percentage. Solid content percentage does not affect to stability in this case.
- Experimental design shows that milling time has an important influence, because as can be observed, a higher milling time always provides a bigger stability for the same dispersant percentage. It can be seen in *Graphic 4-3*:

EFFECT OF MILLING TIME IN STABILITY



Graphic 4-3. Effect of milling time in Δ BS (%) 24h for different dispersant percentage
Milling time of 60 minutes is black line and 90 minutes is blue line

Beforehand, increased milling time should reduce particle size distribution of suspensions. It causes that dispersant effect would be higher in suspensions with 90 minutes of milling time (lower particle size) because steric effects would be better. This reasoning would be correct according to *Graphics 4-2 and 4-3*.

On the other hand, if results obtained for particle size distribution (*Table 4-1*) are observed, the following conclusions are achieved:

- Particle size distribution obtained for each time of grinding was very similar although this one was slightly lower when time of milling was 90 minutes generally.
- It can be affirm that different particle size distribution don't differ significantly due to pre-grinding. So, increase of stability of suspensions doesn't due to milling time of 90 minutes. Therefore, the above explanation isn't correct.

In order to find a correct explanation about increase of stability against sedimentation for compositions milled 90 minutes, graphics obtained by Turbiscan for compositions milled at 60 minutes (*Figure 4-4*) and 90 minutes (*Figure 4-5*) were observed.

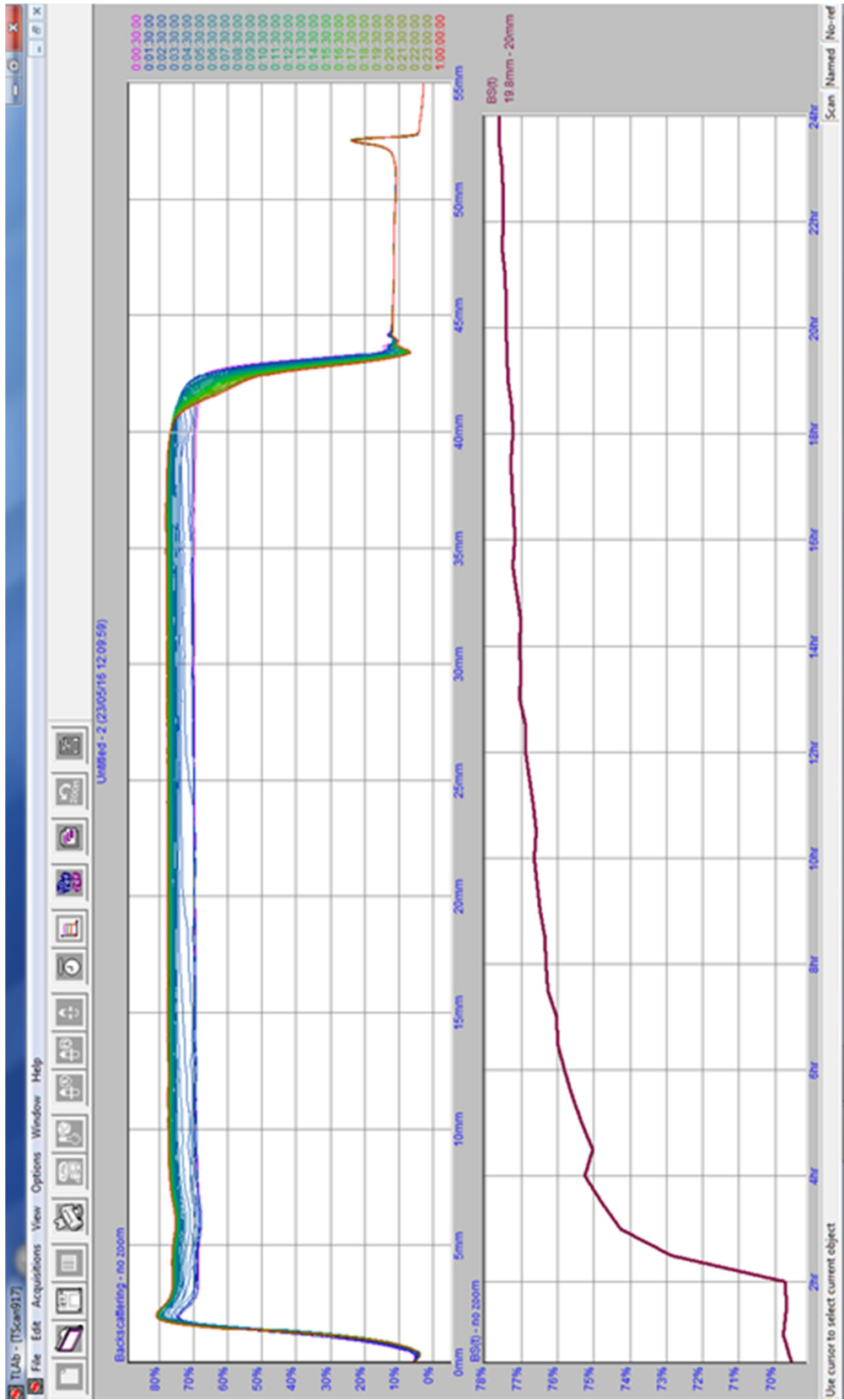


Figure 4-4. Composition 5 milled at 60 minutes

Figure 4-4 shows two different graphics obtained by Turbiscan for composition 5 which was milled at 60 minutes.

- The top graph is a representation of percentage of backscattering front height of the cuvette.
- The chart below is a representation of percentage of backscattering front time for a height of cuvette of 19.810 to 20.019 mm.

On top chart it can be seen that a large increment of backscattering in central zone of cuvette was produced for a determined time. It seems that larger particles unknown deposited in the bottom of cuvette and their higher particle size distribution does not appear in Mastersizer because there is low quantity of them.

This behavior is reflected in graph below, large particles cause a quickly increment of backscattering between 2 and 4 hours. This increment is stable from 8 hours.

The same two charts can be seen in Figure 3 for composition 4 which was milled at 90 minutes, in this case. On top graph, a large increase of backscattering can't be observed. Increment of backscattering for a height of cuvette of 19.810 to 20.019 mm was progressive during the time in chart below.

According to graphics obtained by Turbiscan, it is possible to give an explication for the increase of stability against sedimentation for compositions milled 90 minutes. The reason of this increase is that particle size distribution of particles unknown was reduced for 90 minutes of milling time. The particle size distribution of these particles for 60 minutes is higher and it produces the increase of backscattering, which is not observed for 90 minutes.

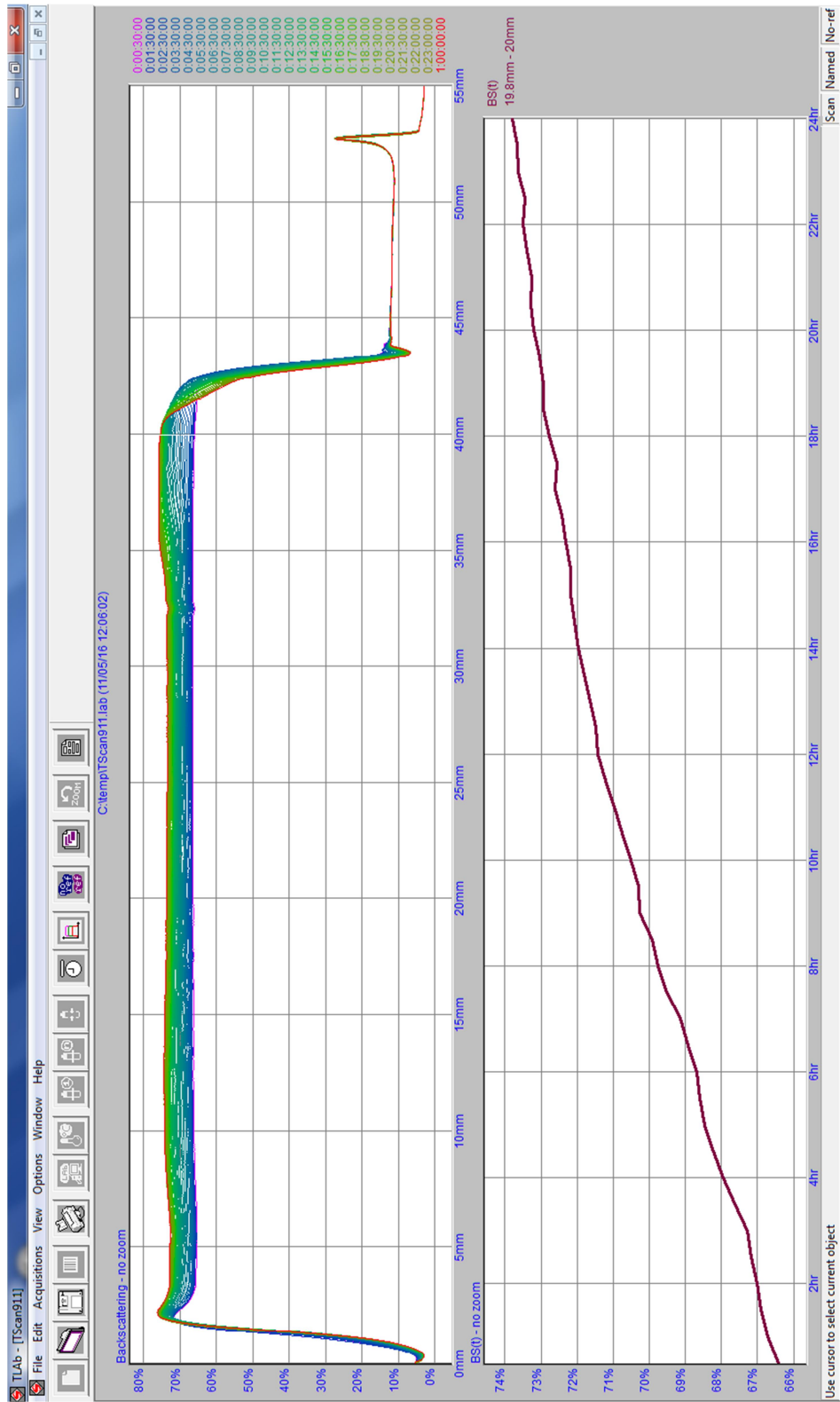
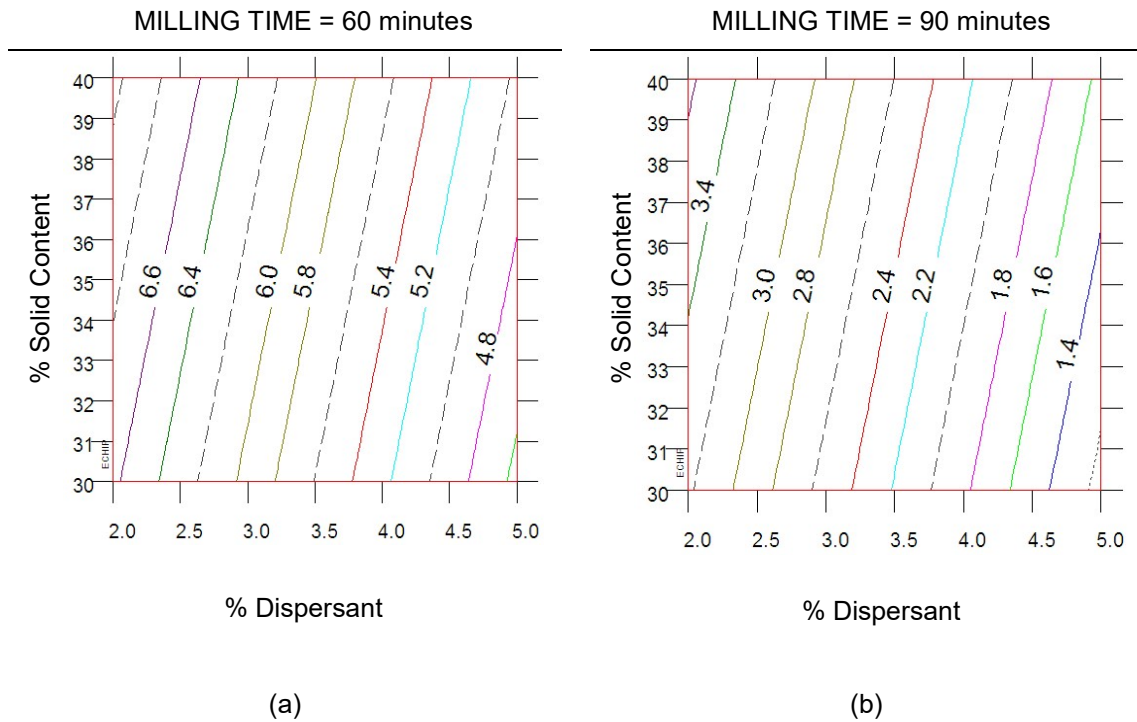


Figure 4-5. Composition 4 milled at 90 minutes

Stability against sedimentation was measured for 8 hours in order to characterize this behavior which has been mentioned above.

Stability against sedimentation: Δ BS (%) 8h



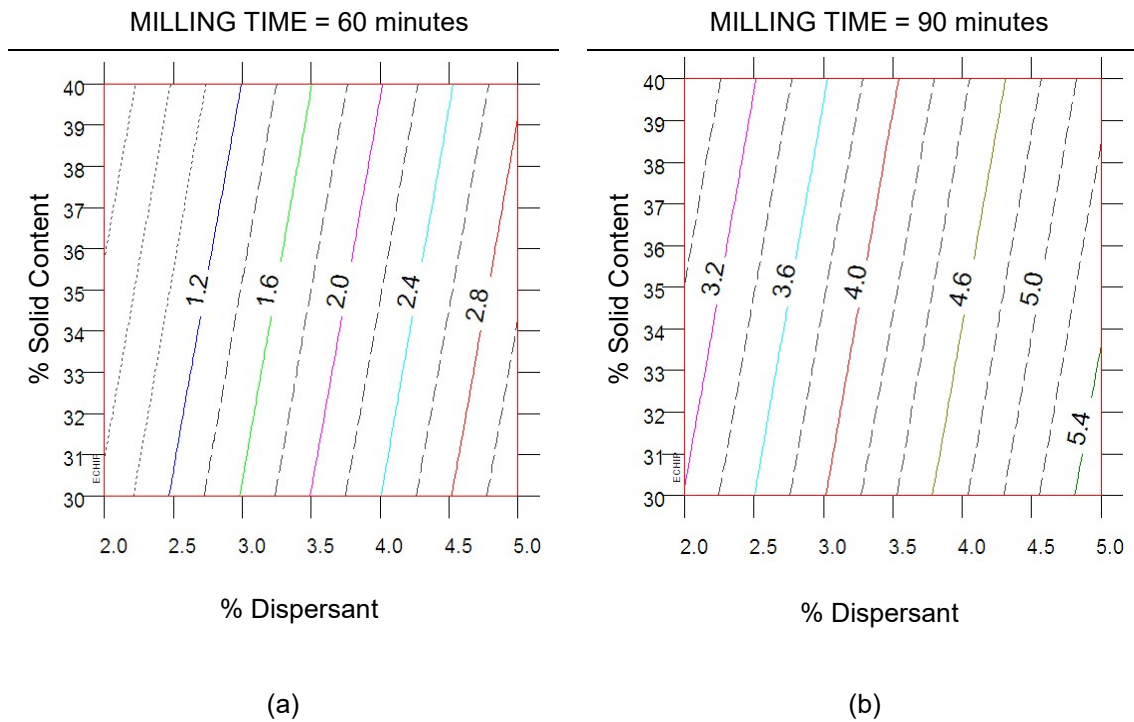
Graphic 4-4. (a) Δ BS (%) 8h tendency for 60 minutes of milling time and (b) Δ BS (%) 8h tendency for 90 minutes of milling time

It can be checked from *Graphic 4-4*:

- Milling time has influence in stability against sedimentation as it has seen from *Graphic 4-2*. This influence is more notable at 8 h than at 24 h for the same composition.

This behavior has seen previously in graphics obtained by Turbiscan (*Figure 4-4* and *4-5*).

Start of sedimentation



Graphic 4-5. (a) Start of sedimentation for 60 minutes of milling time and (b) Start of sedimentation for 90 minutes of milling time

The following conclusions can be obtained from *Graphic 4-5*:

- Higher amount of dispersant provides a higher stability against sedimentation, while solid content does not affect to it.
- It can be observed that milling time has influence in the start of sedimentation. Start of sedimentation begins later when milling time is 90 minutes.
- Start of sedimentation is related to ΔBS (%) directly. When ΔBS (%) is lower, the start of sedimentation is higher.

Experimental error

As had previously seen, experimental error was checked by composition of suspension 1. It was prepared and was characterized two times. Numeric value of different properties for two compositions is below (*Table 4-8*):

Table 4-8. Experimental error for the different compositions 1

| Properties | Viscosity (cP) | Pseudoplasticity Index (cP) | d90 (µm) | ΔBS (%) 24h | ΔBS (%) 8h | S _{sed} (h) |
|--------------------|----------------|-----------------------------|----------|-------------|------------|----------------------|
| Composition 1 | 24.411 | 0.749 | 0.406 | 4.5 | 1.7 | 5.5 |
| Composition 1' | 25.028 | 0.897 | 0.420 | 3.4 | 1.3 | 4.5 |
| Mean | 24.720 | 0.823 | 0.413 | 4.0 | 1.5 | 5.0 |
| Standard deviation | 0.440 | 0.105 | 0.010 | 0.8 | 0.3 | 0.7 |

The numeric value of different properties was introduced in ECHIP and then, the program is able of calculated the mean and the standard deviation of the measurements of composition 1 and 1'.

In this experimental design (lineal design), it doesn't seem important, because standard deviation only can be calculated for one composition. However, if experimental design is more difficult, ECHIP avoids performing a lot of calculations.

From standard deviation of composition 1, this software can calculate the predictions for all compositions. Predictions can be observed in *Table 4-9*. These predictions are very important in order to optimize this experimental design.

Table 4-9. Predictions

| Compositions | Viscosity (cP) | Pseudoplasticity Index (cP) | d90 (µm) | ΔBS (%) 24h | ΔBS (%) 8h | S _{sed} (h) |
|--------------|----------------|-----------------------------|----------|-------------|------------|----------------------|
| 1 | 24.59 | 0.786 | 0.416 | 4.3 | 1.6 | 5.1 |
| 2 | 16.04 | 0.285 | 0.362 | 8.2 | 6.6 | 0.8 |
| 3 | 20.24 | 0.501 | 0.401 | 5.4 | 4.6 | 3.2 |
| 4 | 20.39 | 0.570 | 0.377 | 7.1 | 3.6 | 2.8 |
| 5 | 19.99 | 0.565 | 0.377 | 8.8 | 7.1 | 0.4 |
| 6 | 20.63 | 0.506 | 0.401 | 3.6 | 1.1 | 5.6 |
| 7 | 16.43 | 0.290 | 0.362 | 6.4 | 3.2 | 3.2 |
| 8 | 24.20 | 0.781 | 0.416 | 6.1 | 5.0 | 2.8 |
| 9 | 20.12 | 0.533 | 0.389 | 7.1 | 5.8 | 1.8 |
| 10 | 20.51 | 0.538 | 0.389 | 5.4 | 2.4 | 4.2 |

4.3. Optimal Composition of Experimental Design

Once experimental design is done and all properties and their variations are studied in function of defined variables, it is time of establish a series of conditions in order to find the optimal composition of experimental design.

Conditions imposed in this case can be seen in *Table 4-9*:

Table 4-9. Conditions imposed to find optimal composition

| Properties | Optimal | Importance* |
|------------------------|---------|-------------|
| Viscosity | 20 cP | 3 |
| Pseudoplasticity Index | Minimum | 1 |
| d ₉₀ | - | - |
| ΔBS (%) 24h | Minimum | 1 |
| ΔBS (%) 8h | - | - |
| S _{sed} (h) | Minimum | 1 |

*Values of importance: 1 is the minimum importance and 3 is the maximum importance.

The data shown in *Table 4-9* were introduced in ECHIP and the prediction of optimal composition by program was the next (*Table 4-10*):

Table 4-10. Optimal Composition

| % Dispersant | % Solid Content | Milling Time (minutes) |
|--------------|-----------------|------------------------|
| 4.6 | 30 | 60 |
| 4.6 | 30 | 90 |

In addition, software also predicts the value of properties and their interval of variation of optimal compositions (*Table 4-11* and *4-12*):

Table 4-11. Value and interval of variation for properties of composition milled 60'

| Property | Viscosity (cP) | Pseudoplasticity Index (cP) | d ₉₀ (μm) | ΔBS (%) 24h | ΔBS (%) 8h | S _{sed} (h) |
|-------------|----------------|-----------------------------|----------------------|-------------|------------|----------------------|
| Measurement | 19.68 | 0.472 | 0.396 | 5.8 | 4.8 | 2.9 |
| Interval | 17.15-22.21 | 0.262-0.682 | 0.340-0.452 | 3.8-7.7 | 3.6-6.1 | 0.5-5.2 |

Table 4-12. Value and interval of variation for properties of composition milled 90'

| Property | Viscosity (cP) | Pseudoplasticity Index (cP) | d ₉₀ (μm) | ΔBS (%) 24h | ΔBS (%) 8h | S _{sed} (h) |
|-------------|----------------|-----------------------------|----------------------|-------------|------------|----------------------|
| Measurement | 20.07 | 0.477 | 0.396 | 4.0 | 1.4 | 5.2 |
| Interval | 15.56-22.59 | 0.268-0.686 | 0.340-0.451 | 2.1-6.0 | 0.2-2.6 | 2.9-7.6 |

4.4. Results of the Optimal Composition and Interpretation

Composition shown in *Table 4-10* was prepared and it was milled 60' and 90' according to Step 1 and 2. Then, both compositions were characterized according to Step 3. Results obtained for the different properties were (*Table 4-13*):

Table 4-13. Results of optimal composition

| | Milling time | |
|------------------------------------|--------------|------------|
| | 60 minutes | 90 minutes |
| Viscosity (cP) | 20.524 | 20.958 |
| Pseudoplasticity Index (cP) | 0.394 | 0.419 |
| d₉₀ | 0.336 | 0.319 |
| ΔBS (%) 24h | 8.5 | 7.4 |
| ΔBS (%) 8h | 7.2 | 3.1 |
| S_{sed} (h) | 2 | 3.5 |

The interpretation of results is the following:

- The viscosity and pseudoplasticity index are in the range proposed by ECHIP due to that the higher importance was given to viscosity. Pseudoplasticity index is closely related to the viscosity. That's why that pseudoplastic index is minimum as it was expected.
- The value of the particle size distribution is outside the range and it is due to balls of milling used in this grinding which are less deteriorated than when other grindings were carried out.
- It is difficult to predict because each mill, grinding balls or solid (alumina) have a different behavior. Hence, it is a parameter which is complicated of quantify. In addition, if the deterioration of grinding balls is introduced in the experimental design like a control variable, the design would have been very long.
- The value of increases backscattering (%) is also outside the ranges predicted. Perhaps it is due to that the importance of stability is 1 (versus 3 for the viscosity). It may is due to unknown particles which have had a larger particle size. That is milling time affects to stability and particle size distribution affects in this case, too.
- Start of sedimentation is inside of the range.

The properties such as surface tension or density are not characterized because they were not introduced in the mathematical model adjustment.

5. CONCLUSIONS

- Experimental design was performed satisfactorily through ECHIP software and 10 different formulations of an effect ink with alumina were studied.
- The evaluation of the properties of the different formulation disclosed the relationship between response properties and control variable:
 - Particle size distribution did not depend on any control variable and neither of the milling time. It was due to pre-grinding performed.
 - Rheological behavior was affected by percentage of dispersant and percentage of solid content.
 - Surface tension was always the same because it depends on vehicle used and it was the same all the time.
 - Density only was affected by percentage of solid content.
 - Stability against sedimentation was affected by percentage of dispersant and by milling time. Although it really was not for the milling time, but by large particles of unknown origin.
- Optimum composition proposed by ECHIP according to imposed conditions was performed. It is possible to obtain an ink with the desired rheological behavior through the experimental design performed. But, it is not possible to obtain an ink with desired stability front sedimentation, in this case. Perhaps the composition could have been prepared and characterized again.
- In order to improve the experimental design and the optimum composition it is possible to perform a design more complex. Considering that linear design with central point is the simplest design.
- This work done has allowed me to study thoroughly the field of inkjet inks and to learn characterization techniques and equipment such as MASTERSIZER, Turbiscan, rheometer, pycnometer, tensiometer and LABSTAR mill.

SUPPLEMENTARY MATERIAL

1. Characterization of Particle Size Distribution

Particle size distribution was determined by a MASTERSIZER 2000 laser diffraction equipment of MALVERN. In this equipment, particles pass through a laser beam and scattering the light which is collected in the detectors.

The particles scatter light in all directions resulting in a characteristic "light scattering pattern", which depends on the size, shape and optical properties of the particle.

The calculations were performed with the software built into the equipment, using the Mie Theory for interpreting the light scattering signal collected by the detectors.

Mie Theory

It assumes the following considerations:

- The particle is an optical homogeneous sphere and its real and imaginary (absorption coefficient) indices refractive are known.
- The spherical particle is illuminated by a plane wave of infinite extent and known wavelength.
- The real index of refraction of the medium surrounding the particle is also known.

This theory is often used for particles smaller than 50 micrometers

The calculations were made considering the refractive index of the particles of 1.770 and a value of the absorption coefficient of 1.000. As refractive index of the dispersing medium (Printojet) it was used 1.436.

Each suspension is dispersed in printojet to a suitable concentration for performing the measurement. The samples are subjected to mechanical agitation and ultrasonication for 15 minutes before carry out the measurement.

The following results were obtained for each of the different compositions: d_{10} , d_{50} and d_{90} (μm).

2. Characterization of Rheological Behavior

The measurement of rheological behavior was performed with a CVO-120 HR BOHLIN rheometer, which controls the shear rate or shear stress applied and deformation produced is measured.



Figure 1. CVO-120 HR BOHLIN rheometer

This equipment uses an air bearing system which induces a minimum friction, thus sensibility is maximum. Sample is kept at 25 °C during testing. Double gap geometry is employed to ensure high sensibility with low viscosity suspensions. It can be observed in *Figure 1*.

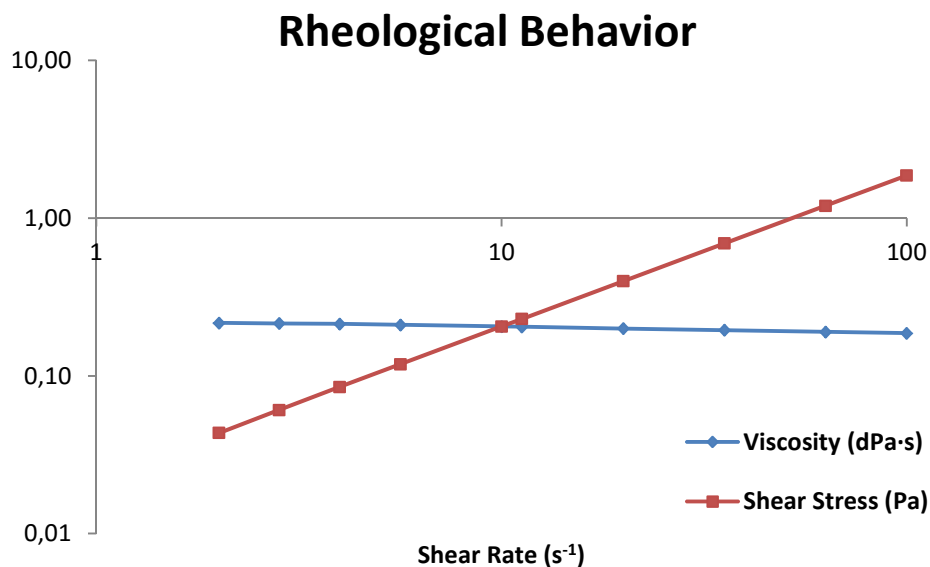
Flow tests were programmed with software and they consisted in the sequence of steps which are described next:

- 1-Vigorous stirring with high velocity (Shear rate = 100 s^{-1} during 30 seconds).
- 2-Rest period (60 seconds).
- 3-Velocity gradient. Increasing logarithmic ramp of shear rate was applied.

An example of data and curves obtained by rheometer software can be observed in *Table 1* and *Graphic 1*, respectively.

Table 1. Results of Rheological Behavior

| Time t (s) | Temperature T (°C) | Target Shear Rate $\dot{\gamma}_T$ (s ⁻¹) | Shear Rate $\dot{\gamma}$ (s ⁻¹) | Percentage Deviation % _{dev} (%) | Shear Stress σ (Pa) | Viscosity η (Pa·s) | Normal Force Thrust (g) |
|------------|--------------------|---|--|---|----------------------------|-------------------------|-------------------------|
| 60.0 | 24.9 | 2.0000e+00 | 2.0080e+00 | -0.40 | 4.3474e-02 | 2.1650e-02 | 0.5 |
| 111.6 | 24.9 | 2.8245e+00 | 2.8246e+00 | -4.3432e-03 | 6.0682e-02 | 2.1483e-02 | 0.5 |
| 156.9 | 25.1 | 3.9888e+00 | 3.9839e+00 | 0.12 | 8.5109e-02 | 2.1363e-02 | 0.5 |
| 197.8 | 25.1 | 5.6332e+00 | 5.6306e+00 | 0.05 | 1.1848e-01 | 2.1042e-02 | 0.6 |
| 234.0 | 25.1 | 1.0014e+01 | 1.0007e+01 | 0.06 | 2.0571e-01 | 2.0556e-02 | 0.6 |
| 269.7 | 24.9 | 1.1235e+01 | 1.1228e+01 | 0.06 | 2.2967e-01 | 2.0454e-02 | 0.5 |
| 303.0 | 24.9 | 1.9972e+01 | 1.9968e+01 | 0.02 | 3.9879e-01 | 1.9972e-02 | 0.7 |
| 335.1 | 24.9 | 3.5504e+01 | 3.5504e+01 | -2.0983e-03 | 6.9150e-01 | 1.9477e-02 | 0.7 |
| 366.3 | 25.0 | 6.3112e+01 | 6.3085e+01 | 0.04 | 1.1986e+00 | 1.8999e-02 | 0.5 |
| 397.2 | 25.0 | 9.9998e+01 | 9.9954e+01 | 0.04 | 1.8622e+00 | 1.8631e-02 | 0.2 |



Graphic 1. Results of rheological behavior

Curves obtained as a result of tests are called flow curve and viscosity curve. They represent shear stress and viscosity in function of velocity gradient. It can be checked that behavior of suspensions is Newtonian because viscosity doesn't change with velocity gradient.

Although rheological curves of inks were measured completely (for all shear rate), all points were not used. Rheological behavior was defined as below:

- **Viscosity** (cP) of suspension was the viscosity obtained at 10.01 s⁻¹ of shear rate.
- **Pseudoplasticity Index** (cP) was defined as:

$$I_{Pseud} = \left| \eta \left(5.663 \text{ s}^{-1} \right) - \eta \left(11.24 \text{ s}^{-1} \right) \right| \quad (1)$$

3. Characterization of Stability against Sedimentation

The measurement of stability of suspensions measures the evolution of a sample at a certain temperature. It is performed by measuring the quantity of transmitted light (T) and backscattered light (BS) of a sample using a Turbiscan Lab Expert of FORMULACTION (*Figure 2*). The principle of the measurement is based on the multiple light scattering.

Turbiscan is an optical scanning analyzer that consists in a detection head which moves up and down along a flat-bottom cylindrical glass cell. The detection head is composed of a pulsed near infrared light source ($\lambda = 800 \text{ nm}$) and two synchronous detectors. The transmission detector receives the light at 180° which goes through the sample, while the backscattering detector receives the light scattered backward by the sample at 45° . The transmission signal dominates in dilute samples, while backscatter signal predominates in concentrated samples.

The detection head scans the entire height of the sample because acquiring transmission and backscattering data every $40 \mu\text{m}$. This equipment can be thermo-regulated from 4 to 60°C , it allow increasing temperature which is the ideal parameter to accelerate destabilization processes, while maintaining realistic testing conditions.

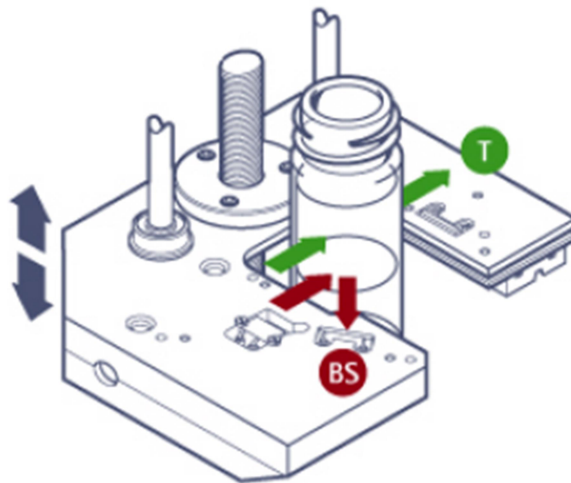


Figure 2. Signals detectors of Turbiscan measurement

An optical scanning was performed for suspensions during 24 hours; measurements were done each 30 minutes. All profiles were obtained, both transmission and backscattering. All tests were carried out at 50°C in order to accelerate destabilization processes.

It is possible seeing destabilization processes from profiles obtained by Turbiscan. But before, it is necessary explain what profile represents (Figure 3).

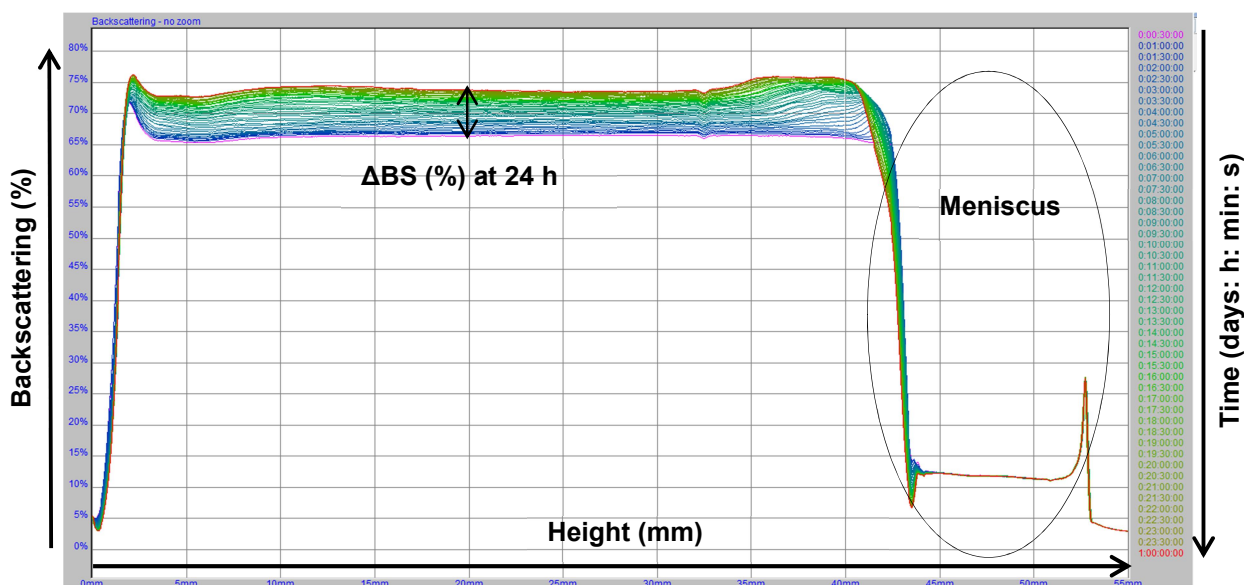


Figure 3. Typical profile of a suspension obtained by Turbiscan

Turbiscan makes scans at various preprogrammed times (each 30 minutes during 24h, in this case) and overlays the profiles on one graph in order to show the destabilization. Graphs are usually displayed in reference mode, whereby the first profile is subtracted to all other profiles, in order to enhance variations. A stable formulation has all the profiles overlaid on one curve, while an unstable product shows variations of the profiles. **Backscattering (%)** is shown in ordinate axes and the **height of the cell** in abscissa axes. In addition, the first profile obtained is displayed in pink, while the last one in red.¹⁹

Stability against sedimentation is quantified by the following parameters:

- **ΔBS (%) at 8 h**

It is measured as an increment of backscattering (%) between backscattering (%) at 8 h and backscattering (%) at 30 minutes (the first profile obtained which is displayed in pink) for a height of cell of 19.810 to 20.019 mm.

- **ΔBS (%) at 24 h**

It is measured as an increment of backscattering (%) between backscattering (%) at 24 h (the last profile obtained which is displayed in red) and backscattering (%) at 30 minutes (the first profile obtained which is displayed in pink) for a height of cell of 19.810 to 20.019 mm. It can be observed in Figure 3.

- **Sediment height (mm)**

It is measured by an option of software.

- **Start sedimentation (h)**

It is measured by the same option of software.

The following profiles (Figures 4 to 6) show the common destabilization processes mentioned in the introduction.

Creaming can be easily detected using a Turbiscan because it induces a variation of the concentration between the top and the bottom of the cell. The following profile (Figure 4) is got:

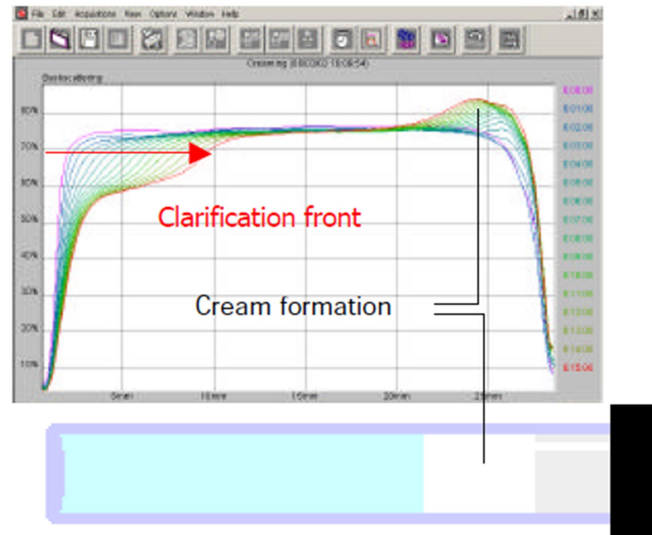


Figure 4. Characteristic profile of creaming

It can be observed (Figure 4) that the backscattering flux decreases at the bottom of the sample due to a decrease of the concentration of dispersed phase in this part (clarification front). Furthermore, it increases at the top of the sample due to an increase of the concentration of the particles (cream formation).

Sedimentation is detected as a variation of the dispersed phase concentration which is produced between the top and the bottom of the sample. The following profile (Figure 5) is obtained by Turbiscan:

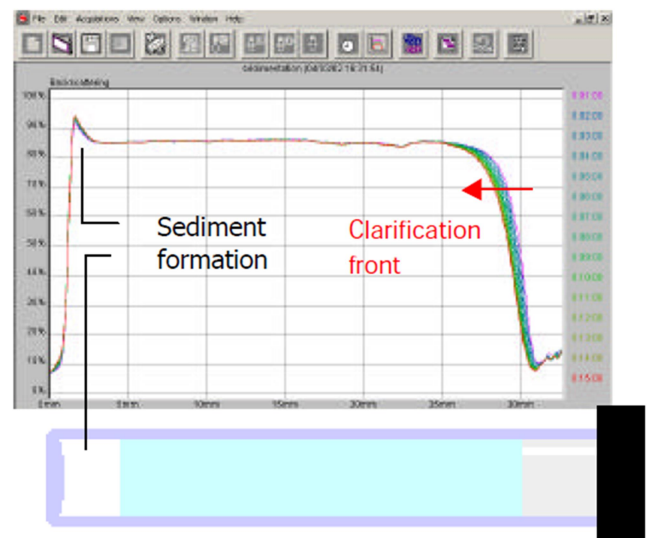


Figure 5. Characteristic profile of sedimentation

Opposite effect is produced; the backscattering flux increase at the bottom of the sample due to an increase of the concentration of dispersed phase in this part (sediment formation) and it decreases at the top of the sample due to a decrease of the concentration (clarification front).

Although **coalescence** and **flocculation** are different phenomena, their behavior is the same regarding the Turbiscan (Figure 6):

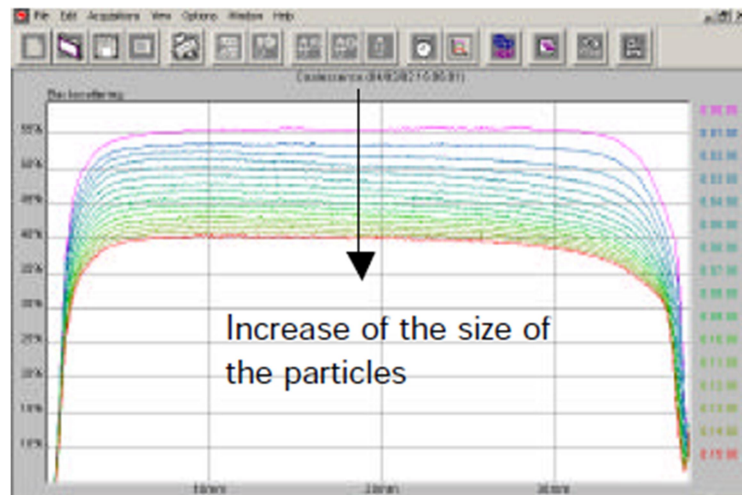


Figure 6. Characteristic profile of coalescence and flocculation

When there is a particle size variation, an increase of backscattering in the middle of the sample is produced.²⁰

4. Characterization of Surface Tension

The determination of the surface tension of the compositions was performed with the K12 tensiometer of Krüss. In this case, the surface tension was determined by static measurements, specifically by plate (Wilhelmy).

WILHELMY PLATE METHOD

The plate method of surface tension measurement requires use of a small rectangle of solid (usually platinum) which is attached to a force measuring system. Dimensions of plate are known and it is vertical. Bottom edge of the plate is made to be straight and parallel to the liquid surface. The liquid which is maintained at 25°C with a thermostatic bath is raised until it just touches the bottom edge of the plate. Force on the plate increases due to wetting of the liquid against the plate. Contact angle between the liquid and the plate is nearly zero (perfect wetting), so the surface tension is easily determined by the following equation:

$$\sigma = \frac{F}{L \cdot \cos \theta} \left(\frac{mN}{m} \right) \quad (2)$$

Where

σ is the surface tension

L is the wetted perimeter of the plate

θ is the angle between the plate and the liquid

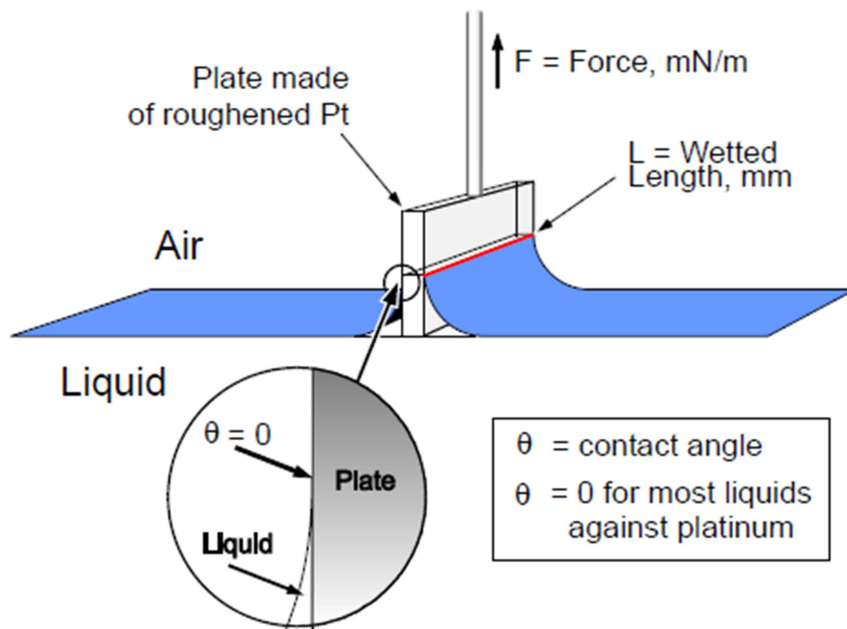


Figure 7. Contact between plate and suspension

5. Characterization of Density

The density of the sample was determined using a pycnometer (*Figure 8*) of 200 g of mass and of 100 cm³ of volume. Once the pycnometer was filled with the sample, its mass (*m*) was determined and the density (*d*) was calculated by the expression below:

$$d(\text{g/cm}^3) = \frac{m - 200}{100} \quad (3)$$



Figure 8. Pycnometer

REFERENCES

1. *A Guide to Ceramic Tile Digital Decoration*. (n.d.). Recovered on September 2, 2016 from <http://www.xaar.com/en/MediaDocuments/Xaar-Ceramic-Guide.pdf>
2. *A Guide to Ceramic Tile Digital Decoration*. (n.d.). Recovered on September 2, 2016 from <http://www.xaar.com/en/MediaDocuments/Xaar-Ceramic-Guide.pdf>
3. *A Guide to Ceramic Tile Digital Decoration*. (n.d.). Recovered on September 2, 2016 from <http://www.xaar.com/en/MediaDocuments/Xaar-Ceramic-Guide.pdf>
4. Paterna, J.J. (2015). *Grupo Esmalglass-itaca: Presente y futuro de la tecnología digital cerámica*. Castellón: XIII Congreso del Técnico Cerámico.
5. *A Guide to Ceramic Tile Digital Decoration*. (n.d.). Recovered on September 2, 2016 from <http://www.xaar.com/en/MediaDocuments/Xaar-Ceramic-Guide.pdf>
6. Knight, E. & Lynn, C. (2010). Understanding Industrial Inkjet Printheads. In E. Knight & C. Lynn, *Industrial Inkjet For Dummies, Xaar Special Edition*. (pp. 9). Hoboken: Wiley Publishing, Inc.
7. Knight, E. & Lynn, C. (2010). Understanding Industrial Inkjet Printheads. In E. Knight & C. Lynn, *Industrial Inkjet For Dummies, Xaar Special Edition*. (pp. 9-11). Hoboken: Wiley Publishing, Inc.
8. *A Guide to Ceramic Tile Digital Decoration*. (n.d.). Recovered on September 2, 2016 from <http://www.xaar.com/en/MediaDocuments/Xaar-Ceramic-Guide.pdf>
9. Knight, E. & Lynn, C. (2010). Understanding Industrial Inkjet Printheads. In E. Knight & C. Lynn, *Industrial Inkjet For Dummies, Xaar Special Edition*. (pp. 11-22). Hoboken: Wiley Publishing, Inc.
10. Magdassi, S. (2010). Inkjet Printing Technologies. In S. Magdassi, *The Chemistry of Inkjet Inks*. (pp. 6-9). The Hebrew University of Jerusalem, Israel: World Scientific.
11. Magdassi, S. (2010). Ink Requirements and Formulations Guidelines. In S. Magdassi, *The Chemistry of Inkjet Inks*. (pp. 22-25). The Hebrew University of Jerusalem, Israel: World Scientific.
12. *Stability analysis with Turbiscan (general cases)*. (n.d.). Recovered on September 10, 2016 from <https://lists.ch.bme.hu/pipermail/oktatok/attachments/20090220/fce7fde4/attachment-0005.pdf>
13. Tadros, T. F. (2010). Principles of Steady-State Measurements. In T. F. Tadros, *Rheology of Dispersions: Principles and Applications*. (pp. 37-42) Weinheim: WILEY-VCH.
14. Magdassi, S. (2010). Ink Requirements and Formulations Guidelines. In S. Magdassi, *The Chemistry of Inkjet Inks*. (pp. 25-26). The Hebrew University of Jerusalem, Israel: World Scientific.

15. Magdassi, S. (2010). Ink Requirements and Formulations Guidelines. In S. Magdassi, *The Chemistry of Inkjet Inks*. (pp. 26-27). The Hebrew University of Jerusalem, Israel: World Scientific.
16. Wheeler, B. & Betsch, R. (2003). *Design of Experiments: Reference Manual* (Version 7). Hockessin: ECHIP, Inc.
17. Wheeler, B., Betsch, R. & Donnelly, T. (2002). *Design of Experiments: User Guide* (Version 7). Hockessin: ECHIP, Inc.
18. *Stability of pigment inkjet inks*. (2009). Recovered on September 11, 2016 from <http://www.titanex.com.tw/doc/tecsupport/ANB-Turbiscan-application%20paper%20on%20%20ink.pdf>
19. *Stability of pigment inkjet inks*. (2009). Recovered on September 11, 2016 from <http://www.titanex.com.tw/doc/tecsupport/ANB-Turbiscan-application%20paper%20on%20%20ink.pdf>
20. *Stability analysis with Turbiscan (general cases)*. (n.d.). Recovered on September 10, 2016 from <https://lists.ch.bme.hu/pipermail/oktatok/attachments/20090220/fce7fde4/attachment-0005.pdf>